THE UNIVERSITY OF ALBERTA

"CLAY MINERALS FROM SOME UPPER CRETACEOUS BENTONITES, SOUTHWESTERN ALBERTA"

A DISSERTATION

SUBMITTED TO THE FACULTY OF GRADUATE STUDIES

IN PARTIAL FULFILMENT OF THE REQUIREMENTS FOR THE DEGREE OF

MASTER OF SCIENCE

FACULTY OF GRADUATE STUDIES

DEPARTMENT OF GEOLOGY

by

WILLIAM ROBERT MAIKLEM B.Sc.

EDMONTON, ALBERTA

MAY, 1962

ABSTRACT

Clay minerals of four bentonites and two shales from Upper Cretaceous continental sedimentary rocks in western Alberta were studied in detail using X-ray diffraction and fluorescence methods. Study of the bentonites was oriented toward appraising their usefulness in correlation. The shales were investigated to help evaluate the influence of depositional environment on clay composition.

The bentonites range in composition from 19 to about 90 per cent mixed layer clay, 3 to 14 per cent kaolinite, no illite or chlorite and from none to almost 80 per cent montmorillonite. The shales lack the mixed layer clay, contain from about 25 to about 50 per cent kaolinite, 40 to 75 per cent montmorillonite, small amounts of illite, and one sample contains some chlorite.

Fourier transforms of the mixed-layer clays show three component interstratifications which in three of the bentonites are within the compositional limits of 50 to 62 per cent illite, 14 to 35 per cent vermiculite and 15 to 30 per cent montmorillonite. The mixed-layer clay from the fourth bentonite contains only 20 per cent illite, 18 per cent vermiculite and 62 per cent montmorillonite which is partly present as a mechanical mixture. Calculations and combination transform peaks suggest a tendency toward a long range ordering of the components.

X-ray spectrochemical analyses checked against wet chemical analyses prove to be promising as a rapid, non-destructive method of determining the major rock forming elements, except Na^{+}, in complex clay systems. At present accuracy of this method limits it to a semi-quantitative analysis. The major chemical components of the four bentonites are quantitatively very

similar. The shales contain more Fe, Mn, Mg and Ti, and less K and Al than the bentonites.

It is concluded that mineralogically the clays may be of use in correlating these bentonites, whereas the chemical compositions are too similar to be used in differentiating them. The shales are mineralogically and chemically different from the bentonites, but similar to one another. Assuming that the shales and bentonites were deposited in similar environments the environment of deposition only slightly modifies the composition of clay minerals.

ACKNOWLEDGEMENTS

The writer wishes to express his gratitude to Dr. J.F. Lerbekmo, under whose direction and guidance this thesis was written, and to Dr. F.A. Campbell for many helpful suggestions. Thanks are due to all staff members of the Department of Geology for their help and encouragement.

The writer would like to acknowledge the generous financial assistance received from National Research Council Grant, A1042, which aided in setting up the standards used in the X-ray fluorescence work.

TABLE OF CONTENTS

TABLES

FIGURES

INTRODUCTION

Thick deposits of Upper Cretaceous strata in the Alberta Foothills are largely continental and difficult to correlate. During the deposition of sandstones and shales, vulcanism in the Cordillera occasionally spread layers of ash, now altered to bentonite beds, over this region. If these bentonites can be traced laterally they will provide helpful time lines for correlation. Original compositional differences in the pyroclastic material ejected will be preserved to some degree in the bentonites. The present study investigates largely the clay mineralogy of four bentonites and two shales at different stratigraphic levels in one section of the Foothills Belly River formation. The study was undertaken as a preliminary investigation into the problem of whether or not the clay mineral composition would aid in characterizing the bentonites.

STRATIGRAPHY

At the beginning of the Upper Cretaceous epoch the present Plains and Foothills region of Western Canada was covered by the Colorado sea, while in the Cordillera to the west, orogenesis was taking place. These opposing conditions controlled the pattern of sedimentation in Western Canada throughout Upper Cretaceous time.

The orogenic area soon became the source of abundant clastic sediments which accumulated as thick deposits of continental sandstones and shales near the western sea shore (Belly River and Edmonton Formations). Oscillation of the shoreline produced an intertonguing of continental and marine sediments within the Foothills and Plains regions of southern Alberta (table 1).

TABLE 1. FOOTHILLS-PLAINS UPPER CRETACEOUS STRATIGRAPHY IN THE REGION OF THE BOW RIVER.

<table>
<tr><th colspan="2">FOOTHILLS</th><th colspan="2">PLAINS</th></tr>
<tr><td colspan="4">EDMONTON FORMATION
(and St. Mary River Formation)</td></tr>
<tr><td colspan="4">BEARPAW FORMATION</td></tr>
<tr><td colspan="4">BELLY RIVER GROUP</td></tr>
<tr><td rowspan="6">ALBERTA GROUP</td><td rowspan="2">WAPIABI FORMATION</td><td colspan="2">LEA PARK FORMATION</td></tr>
<tr><td rowspan="5">COLORADO GROUP</td><td>FIRST WHITE SPECKLED SHALE</td></tr>
<tr><td>WAPIABI FORMATION</td></tr>
<tr><td>CARDIUM FORMATION</td><td>CARDIUM FORMATION</td></tr>
<tr><td rowspan="2">BLACKSTONE FORMATION</td><td>BLACKSTONE FORMATION</td></tr>
<tr><td>SECOND WHITE SPECKLED SHALE</td></tr>
<tr><td colspan="2">BLACKSTONE FORMATION</td><td>BLACKSTONE FORMATION</td></tr>
<tr><td colspan="2"></td><td>FISH SCALE ZONE</td></tr>
</table>

Based on the Petroleum and Natural Gas Conservation Board's "Table of Formations - Alberta" (1960).

The samples used in this thesis were collected by Dr. J.F. Lerbekmo from the Belly River Formation in the Foothills west of Calgary along the Bow River, approximately 1 1/2 miles below the Ghost River Dam (Secs. 17 & 18, Tp. 26, R. 5, W.5th Meridian). At this location approximately 2400 feet of continental Belly River beds are underlain conformably by the marine shales of the Wapiabi Formation and overlain, in fault contact, by the same formation (figure 2).

The marine Bearpaw shale which to the south and east separates the Belly River and Edmonton formations has not been identified in the Foothills at this latitude. Thus the boundary between the stratigraphic equivalents of the Plains Belly River and Edmonton Formations is somewhat uncertain at this locality. To the north the Belly River and Edmonton formations are grouped into the Brazeau and Saunders Formations.

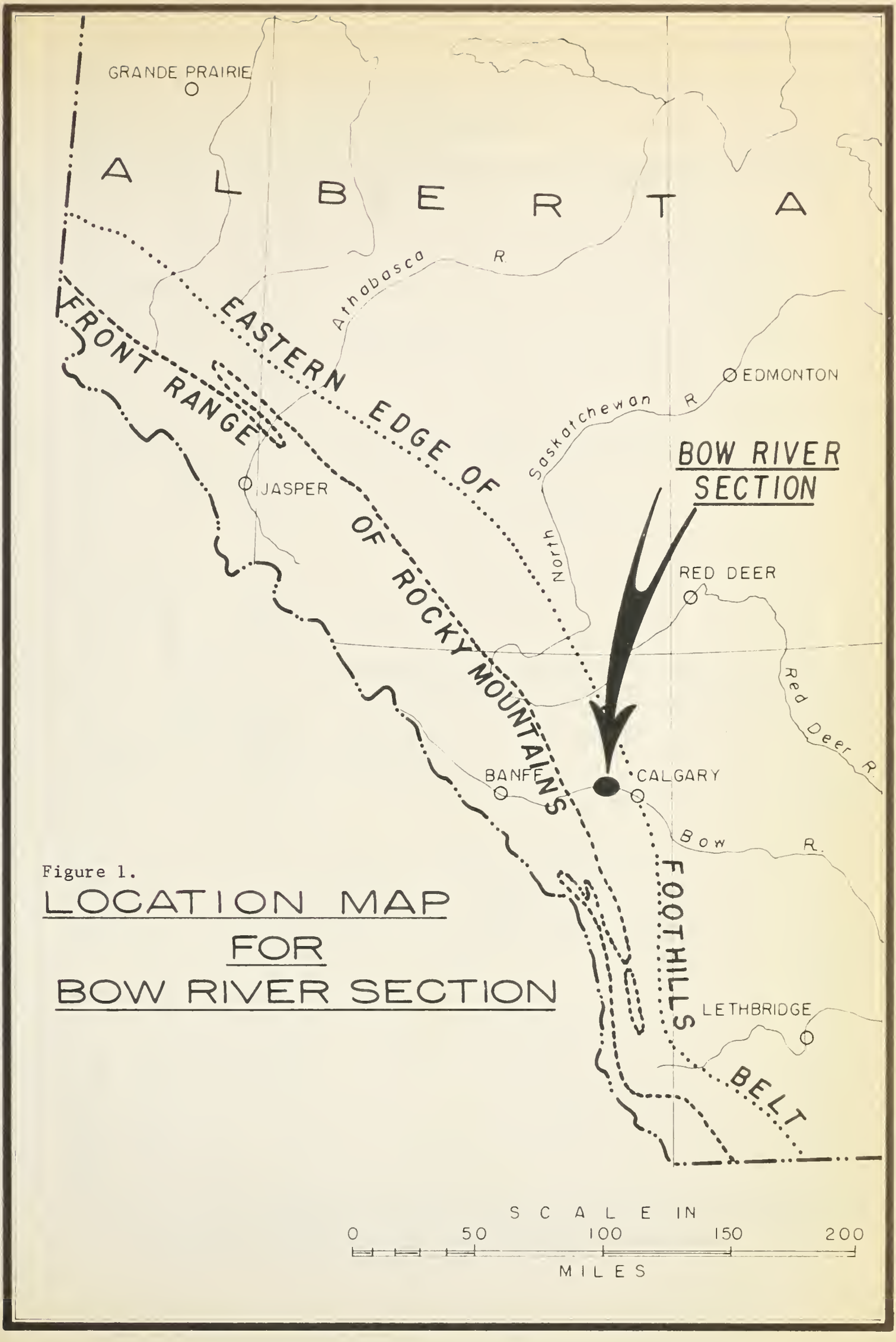

Figure 1.

LOCATION MAP FOR BOW RIVER SECTION

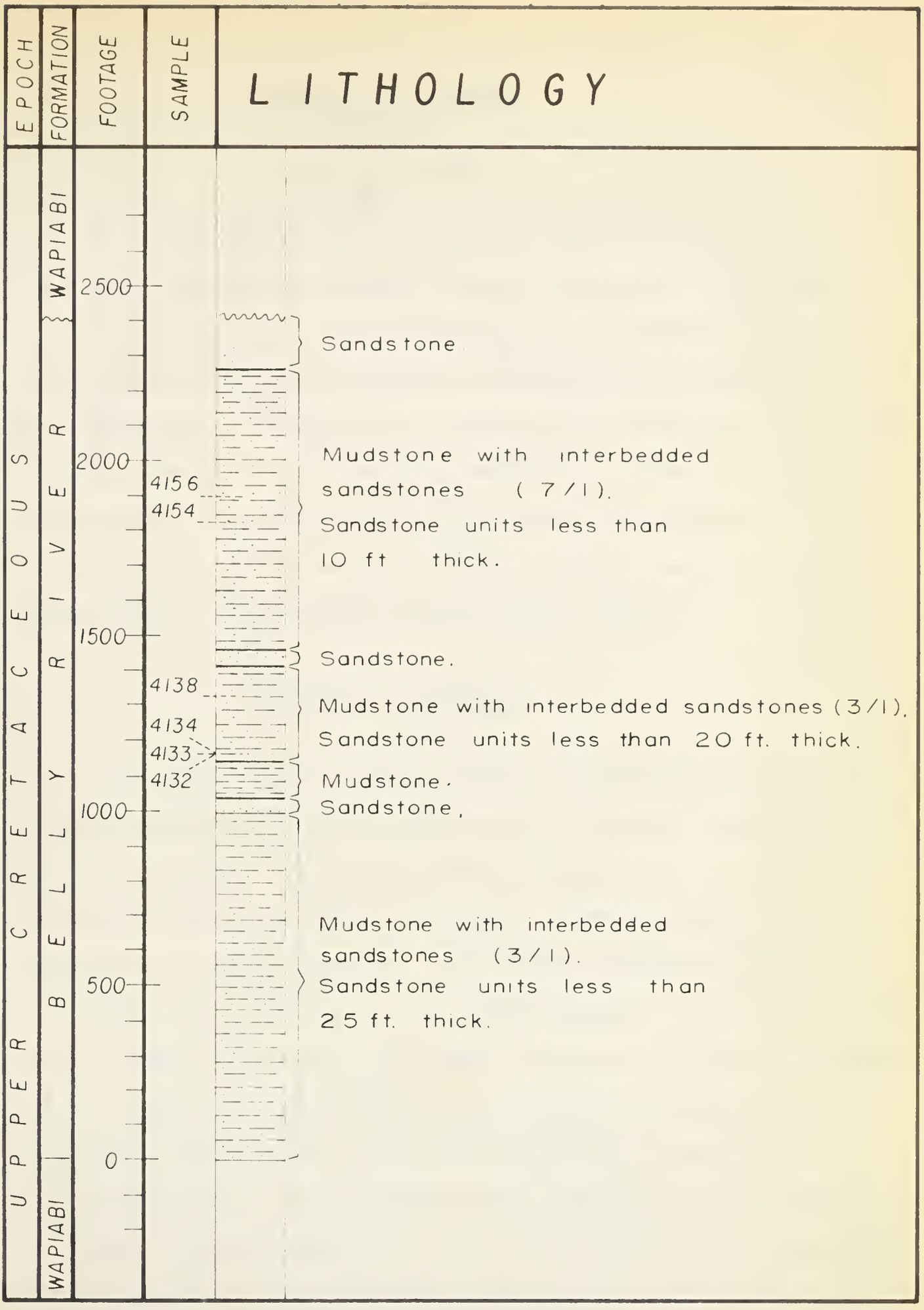

Figure 2. Bow River section of Foothills Belly River Formation. (Sec. 17 and 18; Tp. 26; R. 5; W. 5th M.)

COMPOSITION OF SAMPLES

GENERAL STATEMENT

A detailed compositional analysis was undertaken of four Belly River bentonites and two associated shales. The material coarser than clay size was initially separated and qualitatively examined, but, with the exception of carbonate contents, no quantitative work was done on it. X-ray diffraction techniques were employed in the investigation of the clay fraction. Qualitative and quantitive analyses were attempted including a detailed study of the mixed-layer clays found in the bentonites. X-ray fluorescence was used to determine the major chemical components of the samples, and a comparison made with wet chemical analysis.

MACROSCOPIC DESCRIPTION

The samples used are briefly described in stratigraphic order from oldest to youngest. Bentonite 4132 occurs 1164 feet above the base of the formation and is the lowest one observed in this section. It is 4 inches thick, yellowish to greenish grey in color, slightly calcareous, and is underlain and overlain by shales. The two shale samples were taken from a five foot unit that directly overlies this bentonite. Shale 4133, taken one foot above the bentonite, is a light olive grey. It is well indurated, has an irregular fracture, is calcareous in patches, and contains a 1/4-inch-diameter resin patch. Shale 4134, two feet above the bentonite, is pale yellowish brown, non-calcareous, poorly indurated and very fissile and flaky. The second bentonite, 4138, is 1332 feet above the base of the formation and is 6 inches thick. This bentonite is greenish grey, has a moderate carbonate content and shows some laminations. It also is underlain

and overlain by shale. Bentonite 4154, 1824 feet above the base of the section is 1 foot thick. It is yellowish grey to greenish grey, has a moderate carbonate content, and shows some laminations. It is underlain by coal and overlain by shale. The highest observable bentonite bed in the section, sample 4156, is 1899 feet above the base and occurs in a unit 1 to 2 feet thick. It is various shades of greenish grey with a streak appearance due to the inclusion of carbonaceous material, and is fairly calcareous.

PARTICLE SIZE COMPOSITION

Attempts to make a size analysis of the coarser crystalline material in the bentonites was unsuccessful. The portions of the samples that were coarser than clay size, hereafter referred to as the coarse fractions, were found to be dominantly aggregate particles mostly of silt size, with much smaller portions of sand-size material. These aggregate particles resisted disaggregation in a Waring Blender in a Calgon solution. Smith (1960) noticed that repeated treatments of the sand fraction of such bentonites continuously changes the size distribution. The aggregate grains could be either primary glassy rock fragments or secondary composite grains due to lithification, thus any size analysis which included this material would be strongly suspect. The non-phyllosilicate crystals could not be separated from the aggregate grains by either conventional gravimetric or magnetic procedures, and, therefore, a meaningful size analysis could not be made. The simple two-fold division into clay-sized material and coarser material is shown in table 2. For a detailed account of the procedure followed in this separation the reader is referred to Appendix A.

TABLE 2. FIELD SAMPLE COMPOSITION

Sample	Weight % Clay	Weight % Coarse Fraction	Weight % Carbonate	Weight % Non-soluble Material
4156	77	23	6.7	93.3
4154	68	32	4.0	96.0
4138	89	11	8.2	91.8
4132	~98	~2	7.7	92.3

CARBONATE CONTENT

An estimate of the carbonate content of the bentonites was made by using 20% hydrochloric acid solution to dissolve the carbonate from a small portion of each sample. It is worthy of note that the carbonate content of these bentonites is lowest when the coarse fraction is highest, and vice versa. It thus appears that the carbonate is not associated with the coarse fraction, but rather with the clay or glassy part of the ash fall.

CLAY MINERALOGY

General statement

Clay minerals constitute the major part of bentonites, as shown in table 2. A detailed qualitative and quantitative analysis by X-ray diffraction was undertaken to determine the composition of the clays in the four bentonites studied. It was hoped that this work would show some significant differences between the clay fractions of the bentonites, thus allowing them to be used as an aid in correlation. At the same time, for comparison, the clay fractions from two shales, adjacent to the lower bentonite bed, were

analysed in the hope that they would aid in interpretation of environment and provenance.

X-ray diffraction

Theory and Instrumentation:

The diffraction of X-rays by orientated clay samples was the basic technique employed in this study. Powder film data were also obtained, but only minor use was made of these. A detailed account of X-ray diffraction theory is given by Klug and Alexander (1954) and Henry, Lipson and Wooster (1960).

Standard Norelco X-ray equipment used in this work consisted of a basic X-ray unit, copper X-ray tube ($\lambda_{K\alpha_1}$ = 1.54050Å) and nickel filter, electronic recording panel, strip chart recorder and 114.6 mm X-ray camera. The basic X-ray unit was operated at 35 KV and 15 MA and the goniometer scanned at 1° 2θ per minute. The geiger tube pick-up was operated with a DC power supply of 1500 V. Scale factors, multiplier and time constant were varied to give the best resolution for each sample.

Sample preparation:

A common sample preparation technique in clay mineralogy is to sediment the flaky clay particles from an aqueous suspension onto a glass slide. In samples prepared this way, the "C" crystallographic axes of the clay mineral, being essentially perpendicular to the largest surface of the flake, becomes preferentially orientated nearly perpendicular to the surface of the slide.

Preparation of the samples consisted of letting the clays settle in an aqueous suspension until a 50 ml aliquot of the suspension taken with a pipette from a given depth contained only particles less than 2 μ. This aliquot was then put in a 150 ml beaker containing a frosted glass slide and allowed to sit until all material greater than 1/2 μ had sedimented onto the slide. Most of the remaining fluid was then pipetted off and the slides air dryed.

Unorientated samples for camera work were prepared from a 1/2 μ to 2 μ size-fraction of clay, separated from an aqueous suspension in a similar manner to the orientated samples. In this case the clay was mixed with C-I-L Household Cement and rolled between two glass slides as the cement dried to form a fine spindle. The spindles were mounted directly in the camera.

Analytical procedures:

Each of the orientated samples was X-rayed in its untreated condition, after glycolation and after heat treatment. Glycolation was brought about by placing the slides in a vacuated container with liquid ethylene glycol for 12-15 hours as described by Brunton (1955). Heating was carried out in a Temco Electric furnace at 475° C for 12 hours.

In X-raying the slides the geiger tube scanned from 0° 2θ to 30° 2θ and the X-ray window was opened at 1/2° 2θ. This range covers the basal reflections of the clay minerals, including large spacing peaks, and two quartz peaks which were used as an internal check on the accuracy of the recordings.

In comparing peak intensities, as is necessary in quantitative work, the X-ray energy applied to the sample must be constant. At 4.5° 2θ with 1/4° divergence and scatter slits, the smallest available for this work, the X-ray beam just covers a 20 mm glass slide. Therefore, below this angle,

using a 20 mm glass slide, X-ray energy is progressively lost and intensity measurements are not comparable. To avoid this loss of energy the slides were placed sideways in the holder giving approximately a 40 mm effective width. In this way it was found that intensity measurements could be made down to about 3° 2θ (d=30 Å).

At 2θ angles over 9° the resolution of the peaks becomes poor with 1/4° slits, and 1/2° slits were substituted. However, this constitutes a change in X-ray energy applied to the slide and makes direct comparison of peak intensities between the two regions impossible. To overcome this difficulty a peak, usually the 7Å kaolinite peak, near the border of the two areas was scanned with both the 1/4° and 1/2° slits in position, thus making an energy correction between the two areas possible.

The unorientated samples were X-rayed only in the untreated state. Exposure time was 3 hours with the spindle continuously rotating.

Qualitative clay mineralogy

Basis of identification:

The structures of clay minerals have been described in detail by Grim (1953), Brown (1961) and others, and concisely summarized by Warshaw and Roy (1961). Warshaw and Roy subdivided the layer lattice silicates on the basis of three criteria, two basically structural and one compositional: (1) the numerical combination of tetrahedral silica layers with octahedral brucite or gibbsite layers (1 tetrahedral:1 octahedral, or 2 tetrahedral: 1 octahedral) in the fundamental sheet unit; (2) the cation content of the octahedral layer, either 2 cations per half unit cell (dioctahedral) or 3 cations per half unit cell (trioctahedral); (3) the manner and perfection

of stacking of the fundamental unit (2:1 or 1:1) packets upon each other.

In X-ray diffraction of orientated samples the basal spacing of the fundamental units is measured. It may be used, therefore, to determine criteria (1) and (3). In powder camera work, a measure of criteria (2) can be obtained from 060. Table 3 from MacEwan (1950) indicates the position of 060 for several minerals.

TABLE 3. POSITION OF 060 FOR SOME CLAY MINERALS (MacEwan, 1950)

Position in Å	Mineral
1.485	Kaolinite
1.49-1.52	Dioctahedral micas and montmorillonites
1.525-1.535	Trioctahedral micas and montmorillonites
1.52-1.56	Chlorites
1.533	Chrysotile and antigorite

Structurally the clays can be divided into five groups according to criteria (1) and (2). The kaolinite-septechlorite group are two-layer (1:1) clays with a fundametal basal spacing of 7 Å. The three-layer (2:1) clays have a basic building block with a basal spacing of 9.5 Å. They are divided into three groups according to the material between the 9.5 Å units. The pyrophyllite-talc group contains no inter-layer material, therefore d_{001} = 9.5 Å. The fine hydrous micas or illites contain a layer of K^+ ions between the 9.5 Å layers and therefore d_{001} = 10 Å. The montmorillonites and vermiculites, and some others, have various interlayer cations plus water. If the interlayer cation is Na^+ there is usually one water layer present and d_{001} = 12.5 Å; if the interlayer cation is Ca^{++}

TABLE 4. CLAY MINERAL IDENTIFICATION FROM X-RAY DIFFRACTION PATTERNS OF ORIENTATED CLAY SAMPLES

KAOLINITE:-- In the natural state an integral series of 00ℓ peaks is present with d_{001} = 7 Å. Glycolation does not shift these peaks, but heating to 475° C destroys the mineral.

CHLORITE:-- An integral series of 00ℓ peaks with d_{001} = 14 Å is present in the natural state. The odd-order basal reflections are weak, sometimes making the mineral hard to distinguish from kaolinite. Glycolation very rarely affects the lattice. Heating to 475° C slightly decreases 001 but intensifies the peak, while the lower order peaks show a loss of intensity.

ILLITE:-- An integral series of 00ℓ peaks is present with d_{001} = 10 Å. Neither glycolation nor heating to 475° C affects the position or intensity of the peaks.

MONTMORILLONITE:-- An integral series of 001 peaks which ideally have d_{001} = 12.5 or 15 Å (corresponding to one and two water layers respectively) in the natural state, but may have an intermediate spacing because of unequal hydration of all layers. On glycolating, d_{001} expands to 17 Å; on heating to 475° C it collapses to 10 Å.

VERMICULITE:-- An integral series of 00ℓ peaks with d_{001} = 14 Å in the natural state. On glycolating, d_{001} will expand to about 15.5 Å, rarely more; on heating to 475° C it will collapse to 10 Å.

MIXED LAYER CLAY:-- The composite peak in the natural state has a larger spacing than any of the d_{001} spacings of the above minerals, usually 24-29 Å. It may move on heating or glycolation, depending on the component minerals present. If the peaks form an integral series, the mixed layering is regular, if they do not, it is random.

FIGURE 3* MOVEMENT OF 001** X-RAY DIFFRACTION PEAKS WHEN CLAYS ARE HEATED AND GLYCOLATED

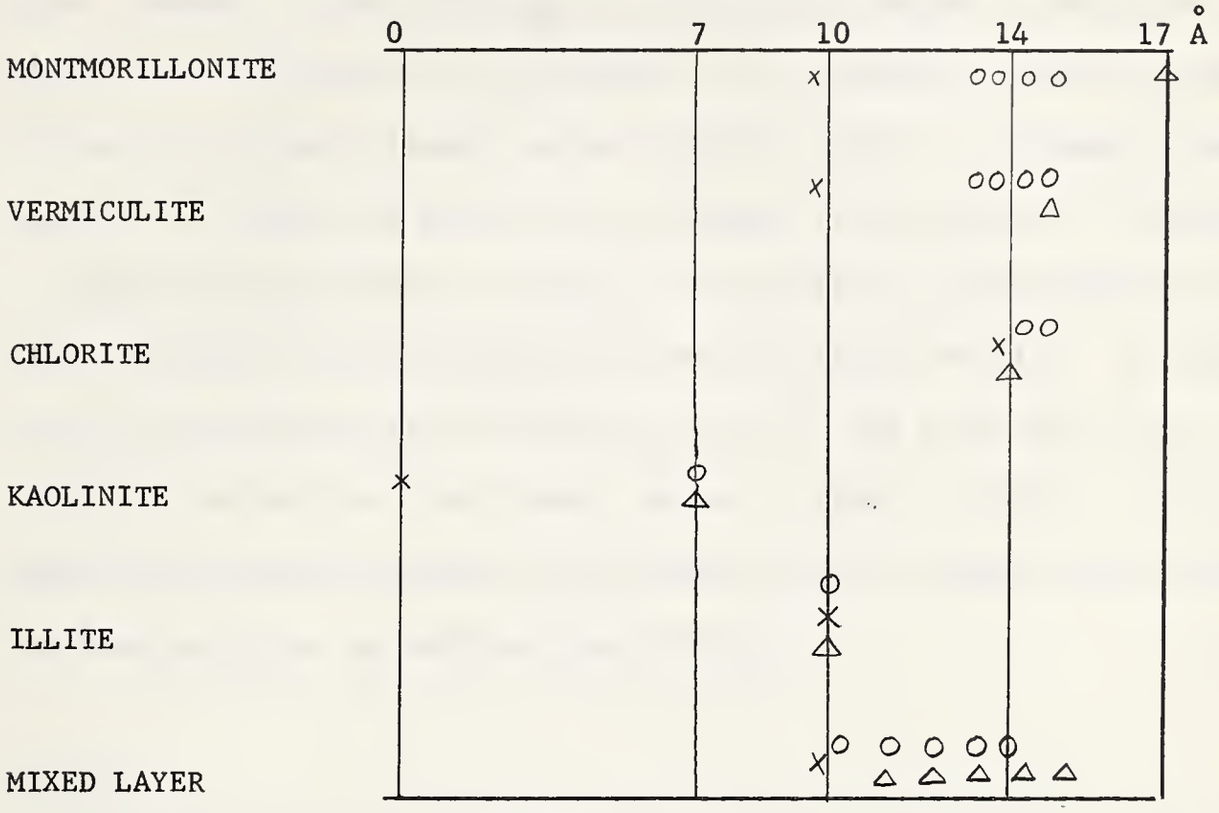

o Untreated

x 475° C

△ Glycolated

*Modified from Weaver (1958) to include vermiculite.

**The Mixed Layer peaks shown are those produced from the combining of the 001 peaks of the clay components present. Weaver (1956) gives such peaks an 001/001 designation.

two water layers are present and d_{001} = 15 Å. Other interlayer cations give spacings near the above two values, depending largely on the state of hydration. Because of the variation of spacing with degree of hydration these minerals are referred to as expandable. The interlayer water may be replaced by an organic liquid such as ethylene glycol, to produce greater expansion, or driven off with heat to collapse the structure. The chlorites or four-layer group have the same 9.5 Å structure as the three-layer minerals plus a brucite or gibbsite layer in the interlayer position. The basal spacing of the resulting four layers is 14 Å. The X-ray data used in differentiating the various clay mineral groups is shown in table 4. Distinction between the minerals within each of these groups is made on the basis of the kind and place of lattice substitution.

Results:

The foregoing criteria for identification were applied to the bentonites and shales under study. The identifications of diffraction peaks (figure 4) are shown in tables 5, 6 and 7.

The double hkl notation after the mixed layer peaks is that used by Weaver (1956). The mixed layer peaks are considered to be the result of scattering contributions from adjacent reflections of the component clays. Thus 002/003 refers to the second order reflection of component A and the third order reflection of component B, both of which contribute to the peak so designated. This notation has been applied here because in the untreated state the three components (see section on mixed layer analysis) have 10 Å, 13 Å, and 13 Å d_{001} spacings, and can thus be treated as a two component 10 Å-13 Å system. In the glycolated state, the three components have d_{001} values of 10 Å, 13 Å and 17 Å and should have a different notation. The notation, however, applied to peaks from glycolated samples is the same as that of the

Figure 4. X-ray diffraction patterns from two orientated clays
a) Untreated
b) Glycolated
c) Heat treated

TABLE 5. IDENTIFICATION OF X-RAY REFLECTIONS FROM UNTREATED SAMPLES

IDENTIFICATION		BENTONITES				SHALES	
MINERAL	hkl	4156	4154	4138	4132	4134	4133
M.L.	composite	27.2Å	26.8Å	29.Å	26.0Å	-Å	-Å
M(a)	001	-	14.2	-	-	13.8	13.8
Chl.	001	-	-	-	-	-	
M(b)	001	-	-	12.8	-	-	-
M.L.	001/001	11.4	11.5	11.6	12.1	-	-
I	001	-	-	-	-	9.9	10.3
M.L.	001/002	-	9.1	8.8	8.8	-	-
M(a)	002	-	7.1	-	-	7.1	7.1
K	001	7.1		7.05	7.1		
Chl.	002	-	-	-	-	-	
M.L.	002/003	4.95	4.95	4.95	5.0	-	-
I	002	-	-	-	-	4.95	4.95
M.L.	020	-	4.48	4.48	4.46	4.50	4.48
M(a)	003	-	-	-	-	-	
Chl.	003	-	-	-	-	-	
Q	100	4.26	4.25	4.24	-	4.26	4.26
Chl.	004	-	-	-	-	-	3.53
M(a)	004	-	3.57	-	-	3.53	
K	002	3.53		3.50	3.56		
Q	101	3.34	3.39	3.34	~3.2	3.35	3.35
M.L.	003/004	3.24					
I	003	-	-	-	-		
fd.		-	3.20	3.18	-	3.2	3.2

M.L. = Mixed Layer
M(a) = 14Å Montmorillonite
M(b) = 12.5Å Montmorillonite
Chl = Chlorite

I = Illite
K = Kaolinite
fd = Feldspar
- = No reflection
Composite = apparent long spacing due to combining of components

TABLE 6. IDENTIFICATION OF X-RAY REFLECTIONS FROM GLYCOLATED SAMPLES

IDENTIFICATION		BENTONITES				SHALES	
MINERAL	hkl	4156	4154	4138	4132	4134	4133
M.L.	composite	29.4Å	32.7Å	28.5Å	31.5Å	-Å	-Å
M.	001	-	17.0	16.7	↖	16.8	16.8
Chl.	001	-	-	-	=17.0	-	14.2
M.L.	001/001	12.9	13.0	13.4	↙	-	-
I.	001	-	-	-	-	9.9	9.9
M.L.	001/002	9.3	9.3	11.6	9.1	-	-
M.	002	-	8.5	-		8.6	-
K.	001	7.1	7.13	7.1	7.1	7.1	} 7.1
Chl.	002	-	-	-	-	-	
M.L.	002/003	5.24	5.24	5.3	5.4	-	-
M.	003	-	-	-	-	5.53	-
I.	002	-	-	-	-	-	5.0
Chl.	003	-	-	-	-	-	} 4.5
M.	020	-	4.46	4.48	4.46	4.46	
Q	100	4.30	4.27	4.24	-	4.26	4.26
M.	004	-	-	-	-	-	4.18
K.	002	3.54	3.57	3.53	3.56	3.53	} 3.53
Chl.	004	-	-	-	-	-	
I.	003	-	-	-	-	} 3.35	} 3.34
Q	101	3.35	} 3.34	} 3.35	-		
M.L.	003/004	3.33			3.35	-	-
M.	005	-	-	-	-	-	3.34
fd.		-	-	-	-	3.2	3.19

M.L. = Mixed Layer
M. = Montmorillonite
Chl. = Chlorite
I. = Illite
K = Kaolinite
fd. = Feldspar
- = No reflection
Composite = apparent long spacing due to combining of components

TABLE 7. IDENTIFICATION OF X-RAY REFLECTIONS FROM HEAT TREATED SAMPLES

IDENTIFICATION		BENTONITES				SHALES	
MINERAL	hkl	4156	4154	4138	4132	4134	4133
Chl.	001	-Å	-Å	-Å	-Å	-Å	13.5Å
"10Å"	001	10.1	9.93	9.8	9.8	9.7	10.0
Chl.	002	-	-	-	-	-	6.6
"10Å"	002	5.01	4.94	4.9	4.9	4.85	5.1
"10Å"	020	-	4.48	4.47	4.47	4.45	4.48
Q	100	-	4.27	4.25	4.25	4.26	4.25
Q	101	-	3.35	3.34	↖	3.34	} 3.34
Chl.	004	-	-	-	3.25	-	
"10Å"	003	3.32	3.29	3.26	↙	} 3.2	3.25
fd.		-	-	3.16			
"10Å"	004	-	2.58	2.55			
"10Å"	005	1.99	1.97				

Chl. = Chlorite
"10Å" = Mixed Layer + Montmorillonite + Illite
Q = Quartz
fd. = Feldspar
- = No reflection

corresponding peaks from the untreated material, so that their movements can readily be followed. A summary of the results of the identifications shown in tables 5, 6 and 7 is given in table 8.

Powder camera patterns for all the bentonites show 060 reflections at 1.50 Å with estimated relative intensity of 80-90 (Appendix F). According to MacEwan (1950, table 3), this value suggests that the minerals reported from the bentonites are all dioctahedral.

Quantitative clay mineralogy

Method:

In determining the proportions of the various clay minerals, a method following Johns, Grim and Bradley (1954), Weaver (1958) and Byrne and Farvolden (1959) was employed. This method is based on earlier work by Bradley (1953). It is well known that the intensity of X-ray diffraction at any given Bragg angle is governed by F, the structure factor, characteristic of the diffracting material; and the trigonometric factor, dependent on the Bragg angle θ. The relationship of the X-ray diffraction intensity, I, to these factors can be expressed as:

$$I = Cst \times F^2 \left(\frac{1 + \cos^2 2\theta}{\sin 2\theta}\right)$$

for orientated clay samples. It is thus apparent that scattering produced from different clays at different Bragg angles will result in peak heights that do not directly represent the proportion of each clay. Using the F values given by Brown (1961), a series of relative intensities can be calculated for the various clay peaks. Correction factors can then be applied to the peak heights so that they will truly represent the amount of each constituent present.

TABLE 8. OCCURRENCE OF CLAY MINERALS IN THE BELLY RIVER BENTONITES AND SHALES

SAMPLE		CLAY MINERAL				
		MIXED LAYER	MONTMORILLONITE	ILLITE	CHLORITE	KAOLINITE
BENTONITES	4156	X	-	-	-	X
	4154	X	X	-	-	X
	4138	X	X	-	-	X
	4132	X	X	-	-	X
SHALES	4134	-	X	X	-	X
	4133	-	X	X	X	X

X denotes occurrence of clay mineral
- denotes absence of clay mineral

Bradley (1953) experimentally determined relative peak intensities for certain montmorillonite-organic liquid complexes (Figure 5). From his work various authors have extracted correction factors. Surprisingly, the correction factors determined from Bradley's work, and those calculated using the standard intensity equation and F values taken from Brown (1961) do not agree, even in order of magnitude. The reason for this discrepancy is unknown and beyond the scope of this study. However, in order that comparison may be made with other studies of this type, it was decided that the correction factors based on Bradley's work would be used in the present investigation.

Johns, Grim and Bradley (1954) point out that the scattering distributions for the various clays is relatively constant in the region d_{001} = 3.3 to 3.5 Å, and thus peaks falling in this region, after a correction for quartz, may be compared directly.

TABLE 9. PEAK INTENSITY CORRECTION VALUES

MINERAL	PEAK	CORRECTION
"10Å"	17 Å	1.0
	15	1.3
	13.4	1.5
	13	1.8
	12.5	1.9
	11.6	2.4
	10	4.0
	9.6	4.7
	9.3	5.7
	9.1	6.3
CHLORITE	7	1.6
KAOLINITE	7	1.6

"10Å" = Montmorillonite, Illite and Mixed Layer Clays.
"10Å" values were read from Figure 5, reproduced from Bradley (1953).
Chlorite and Kaolinite values were determined from Byrne and Farvolden (1959) and Weaver (1958).

Figure 5

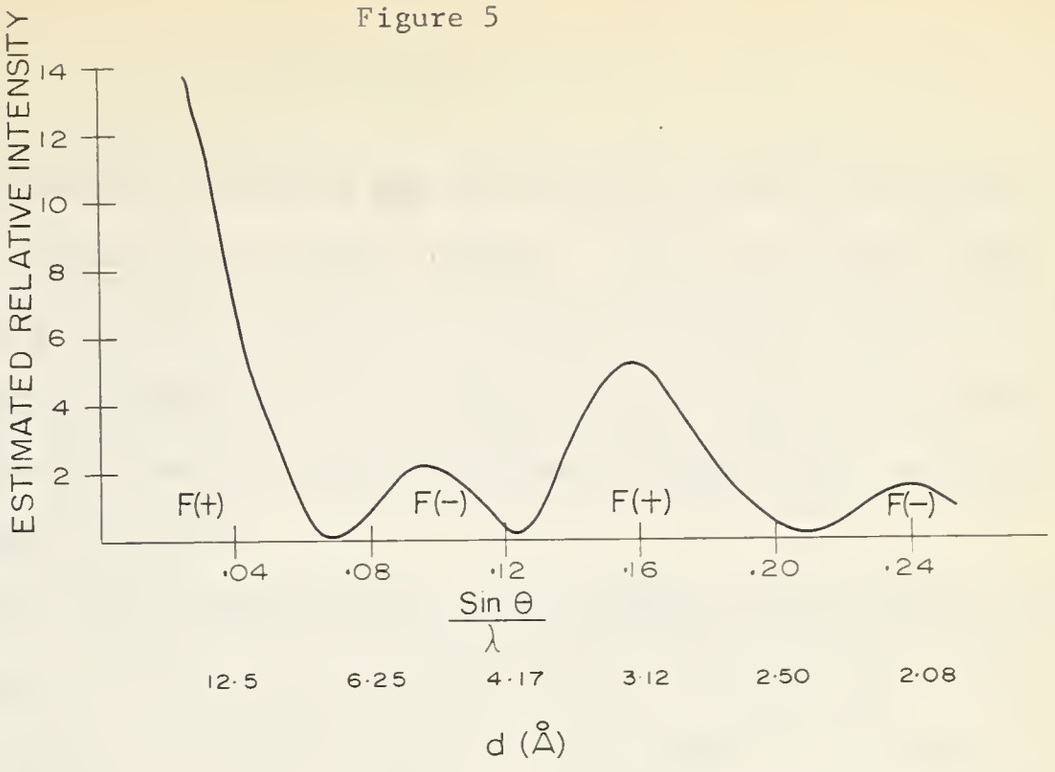

a) Composite curve of relative 00ℓ powder diffraction intensities.
[compiled from montmorillonite-organic complexes by Bradley (1953)]

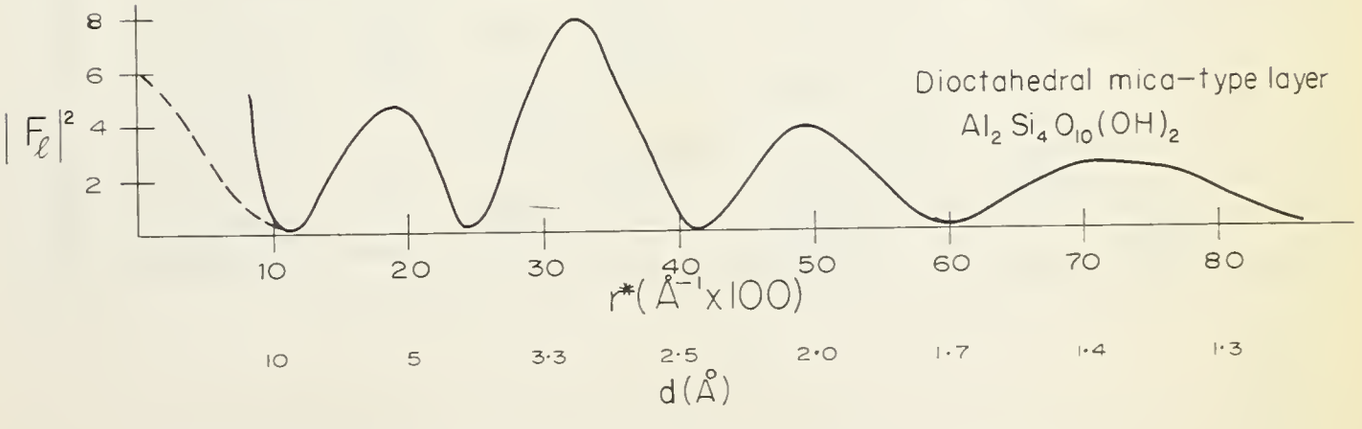

b) Squared moduli of layer structure factor versus the reciprocal lattice**

**From Brown (1961)
r* = 2 sin θ/λ = 1/d

Results:

Quantitative estimates were made using as many of the peaks as possible from the glycolated and natural samples. The results show a range of values. Johns, Grim and Bradley (1954) and Byrne and Farvolden (1959) conclude that his method is accurate to within about five per cent. In the light of the above discussion and the results obtained it appears that the error may be considerably greater.

The results given in Table 10 were taken from calculations using peaks with $d_{001} \geqslant 7$ Å from the glycolated samples. Various combinations of peaks in this region gave similar results. Calculations in the region of d_{001} = 3.3 to 3.5 Å gave variable results, with kaolinite usually being greater than reported here. Similarly, the untreated samples produced variable results, possibly due to a less perfect orientation of the fine montmorillonite and mixed layer material than in the glycolated samples.

TABLE 10. QUANTITATIVE CLAY DETERMINATIONS

	SAMPLE	% CLAY				
		MIXED LAYER	MONTMORILLONITE	ILLITE	KAOLINITE	CHLORITE
BENTONITE	4156	86-87	----	----	13-14	----
	4154	49-52	44-46	----	4-5	----
	4138	19-33	64-78	----	3	----
	4132	93-97		----	3-7	----
SHALE	4134	----	50-57	Trace	43-50	----
	4133	----	42-73		27-58	

Mixed Layer Analysis

Introduction:

The simplest method of mixed layer analysis consists of comparing X-ray diffraction patterns with theoretically calculated patterns, a number of which are presented by Brown and MacEwan (1950) and Brown (1961). This trial and error method has certain limitations: the number of situations for which calculated patterns are available are few; proportions and components may be estimated in this way, but manner of ordering cannot be.

A more direct approach, and the one used in this study, is the Fourier transform method described by MacEwan, Amil and Brown in Brown (1961).

Theory:

For a detailed account of the theory the reader is referred to Brown (1961).

The transforms calculated for the mixed layer clays in this work were done using the series,

$$W_R = \frac{a}{\pi} \sum i(s) \cos (UsR),$$

$$\text{with } i(s) = \frac{Is}{\Theta_s / Fs/2},$$

where W_R is defined as the probability of finding another layer at distance R (measured perpendicularly) from any layer, I_s is the intensity (area under the peak), Θ_s is the trignometric function, $/F_s/^2$ is the squared modulus of the structure factor and $U_s = 4 \sin \theta/\lambda = 2\pi/d_s$. The s subscripts indicate that the values are those from the positions of intensity maximum. θ was taken as $\frac{(1 + \cos^2 2\theta)}{\sin 2\theta}$ and read from tables

in Henry, Lipson and Wooster (1960). $/F_s/^2$ was read from a calculated graph presented in Brown (1961). The one used (Figure 5) was chosen because the minerals present are dioctahedral, and, on heating, all the peaks collapsed to an integral series with d_{001} = 10 Å, indicating a mica-like structure.

On the transforms, Figures 6 and 7, the components have been labled A, B, C, A^2, B^3 etc., where A^2 = AA and B^3 = BBB. The peak heights were calculated on the basis of the sum of the components present being equal to 1. Data used to calculate the transforms is tabulated in Appendix B.

Qualitative analysis:

The components present, which are the same for each sample may be readily identified with the aid of the X-ray diffraction patterns and the two Fourier transforms calculated for each clay. First, the mixed layer X-ray diffraction peaks move on glycolation, indicating the presence of an expandable mineral. Secondly, on heating to 475°C the peaks collapse to form an integral series of 00ℓ peaks with d_{001} = 10 Å indicating the components are basically 10 Å mica-like layers. Examining the transforms of the untreated samples, two components are seen to be present, one with a spacing of 10 Å, the other with a spacing of 12.5 to 13 Å. Comparing the transforms of the untreated samples to those for the glycolated material, the 10 Å component has not moved, and is thus identified as illite (A). The 12.5-13 Å component has split into two peaks, indicating that it consists of two components. The one that expanded to 13.5 Å has been called vermiculite (B), and the other component that expanded to 16.5-17 Å has been identified as montmorillonite (C).

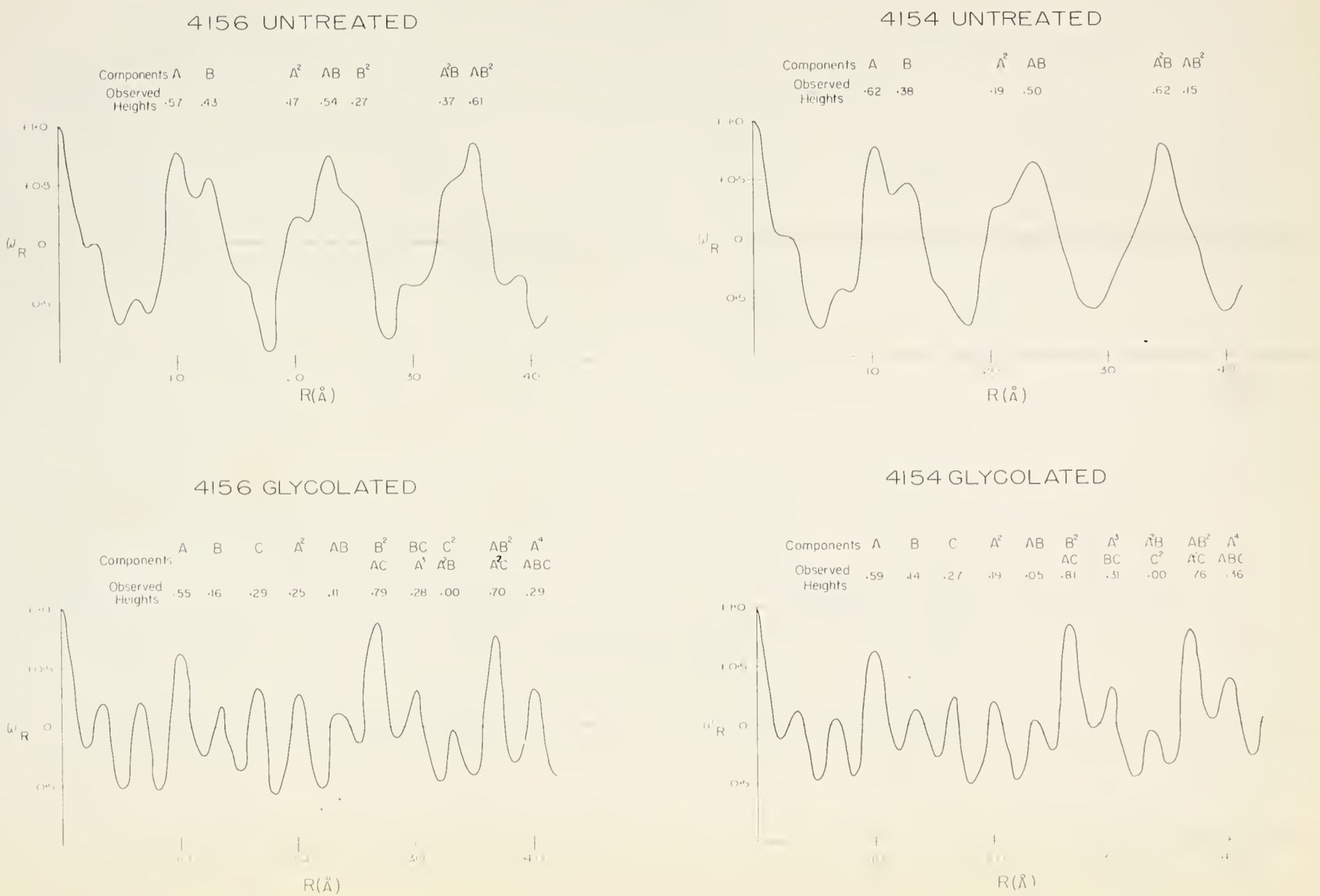

Figure 6. Fourier transforms of mixed-layer clays from bentonites 4156 and 4154

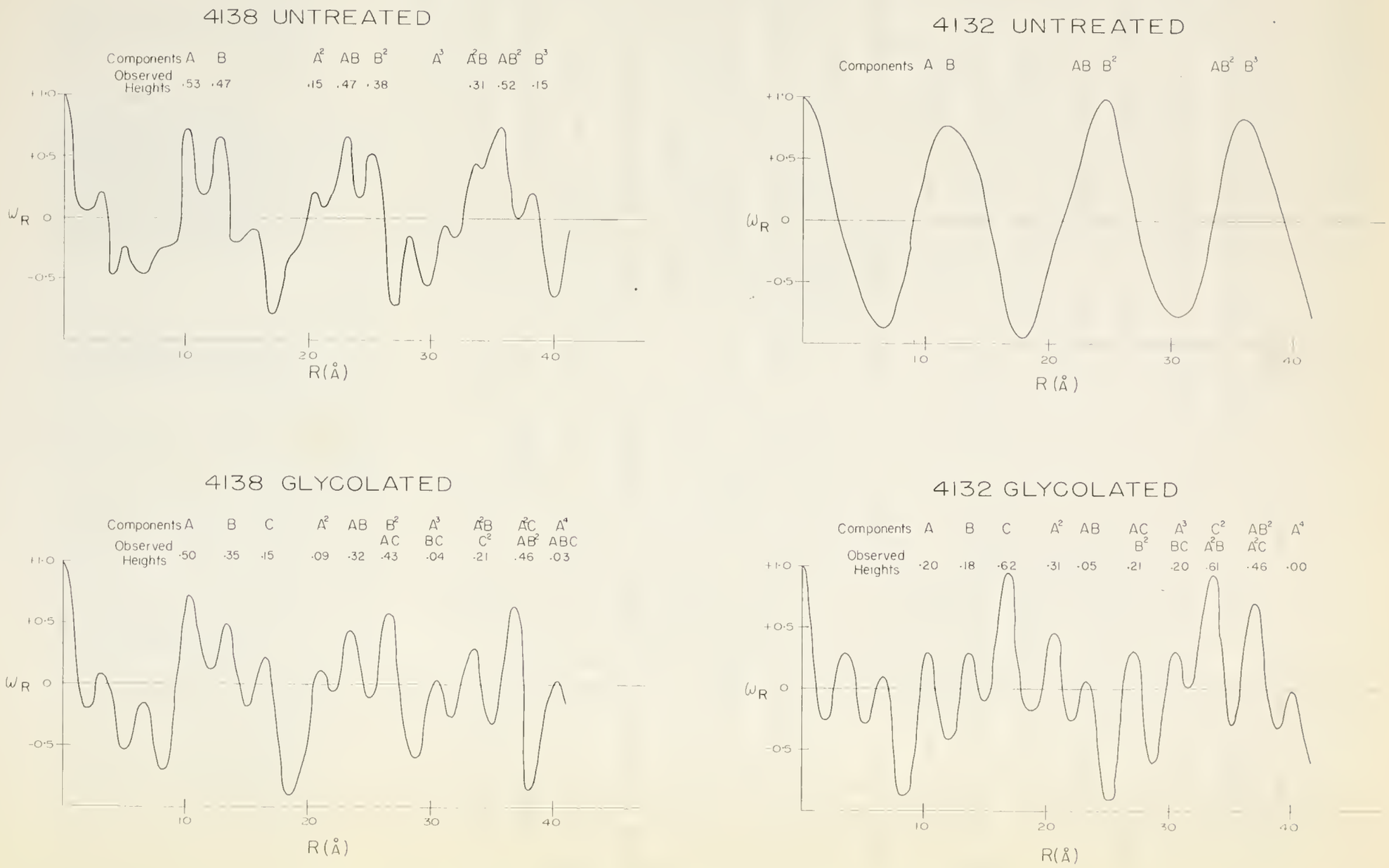

Figure 7. Fourier transforms of mixed-layer clays from bentonites 4138 and 4132

Quantitative Analysis:

In construction of the Fourier transforms it was assumed that every layer would have another layer adjacent to it, that is, the probability of another layer occurring at a distance of 0 Å (R = 0) from any other layer is one. Thus at R = 0, W_R must be one. This condition was met by adjustment of the constant $\frac{a}{\pi}$ in the cosin series. From this it follows that P_A, the probability of component A (or spacing A) occurring, plus P_B, the probability of component B (or spacing B) occurring, when A and B are the only components, must equal one. Also $h_A = P_A$, where h_A is the height of the peak, in terms of W_R, for spacing A. Similarly $h_B = P_B$. It follows from this that $P_A+P_B = h_A+h_B = 1$. The quantities of each component should therefore be directly determinable from the transforms by multiplying the peak heights or probabilities by 100. However, it was found that the direct sum of the component heights was always greater than one. The heights of the peaks given have therefore been adjusted so that their sum does equal one. This was done by dividing all peak readings by the sum of the height of the components. In the case of component A, of the natural samples, the values quoted are therefore h_A/h_A+h_B. The data shown on Figures 6 and 7 are summarized in table 11.

TABLE 11. COMPOSITION OF MIXED LAYER CLAYS

SAMPLE	TREATMENT	% ILLITE	% VERMICULITE	% MONTMORILLONITE
4156	Glycolated	55	16	29
	Untreated	57	43	
4154	Glycolated	59	14	27
	Untreated	62	38	
4138	Glycolated	50	35	15
	Untreated	53	47	
4132	Glycolated	20	18	62
	Untreated	--	--	

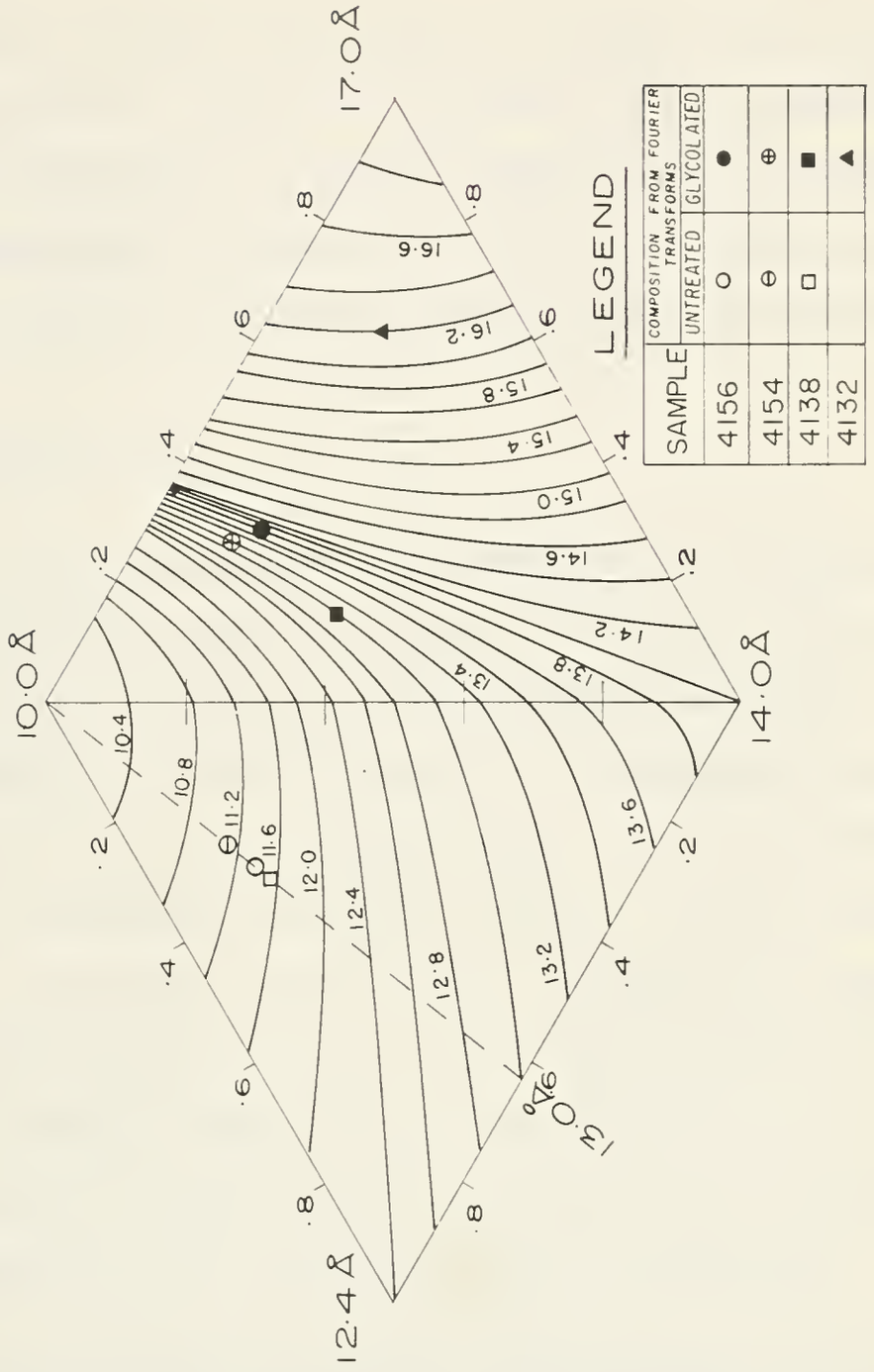

Figure 8. Three component composition triangles

To check the values determined from the transforms, they were plotted on three component composition triangles (Figure 8). The peak positions thus determined and those from the diffraction patterns, in each case, agreed within 1 Å (with the exception of 4132*). This slight discrepancy may be due to one or more of the following: (a) the components of the composition triangles are not precisely those present in the samples, (b) there may be inaccuracies in construction of the composition triangles**, and (c) there are relatively few terms in the calculation of the Fourier transforms.

Interstratification:

For a detatiled account of the methods used in determining interstratification the reader is referred to chapter XI in Brown (1961).

There are three types in interstratification; regular, random and zonal. Regular interstratifications are recognizable because of the integral series of 001 X-ray diffraction peaks. Rectorite (Bradley, 1950) and Allevardite (Brindley, 1956) are two examples. Random interstratification produces a non-integral series of 001 X-ray diffraction peaks. Random mixtures can be compared to packs of cards that have been shuffled. The result would be randomness, that is to say, the probability of any component (card from a particular deck) occurring at any particular position would be equal to the probability of it occurring at any other position.

---

* The reason for the 17 Å spacing in the glycolated X-ray diffraction pattern, essentially that of pure montmorillonite, is not apparent and is discussed under mixed layer analyses. The transform for the untreated 4132 sample is not usable because of the lack of adequate X-ray diffraction peaks in its calculation.

** For construction of the composition triangles the reader is referred to Appendix C.

Interstratification is said to be zonal if separate small units of the minerals occur. Zonal interstratification grades into a mechanical mixture on one hand and into a random interstratification on the other. Similarly, a random interstratification can grade into a regular interstratification.

The various types of interstratifications are most conveniently determined statistically. A, B, C, are designations given to the components present. P_A is defined as the probability (or frequency) of component A occurring, P_B is the probability of B occurring. P_{AB} is the probability that B succeeds A, given that the first layer is A. P_{AA} is the probability that A succeeds A, given that A is the first layer, ---- and so on.

The statistical laws relating the probabilities are given for a system of n types of layers as;

$$\lessgtr_r Pr = 1$$

$$\lessgtr_r Prs = 1 \text{ for all } r$$

$$\lessgtr_r PrPrs = Ps \text{ for all } s$$

The expanded forms of these relations are given in Appendix D. In defining a system it is necessary that these relations are satisfied. However, using these relations it is necessary to give only one quantity to define a two component system; three to define a three component system. The interstratification relationships are defined mathematically for a two component system in table 12 and for a three component system in table 13.

TABLE 12. STATISTICAL DEFINITION OF TYPES OF INTERSTRATIFICATION FOR A TWO COMPONENT SYSTEM WITH $P_A \leq P_B$

Maximum degree of alternation	$P_{AA} = 0$
Partially random interstratification with a tendency to alternation	$0 < P_{AA} < P_A$
Random interstratification	$P_{AA} = P_A$
Partially random; tendency toward zonal structure	$P_A < P_{AA} < 1$
Mechanical Mixture	$P_{AA} = 1$

TABLE 13. STATISTICAL DEFINITION OF TYPES OF INTERSTRATIFICATION FOR A THREE COMPONENT SYSTEM WITH $P_A \geqslant P_B + P_C$

Maximum degree of alternation	$P_{CC} = P_{CB} = P_{BB} = P_{BC} = 0$
Random interstratification	$P_{AA} = P_A$; $P_{BB} = P_B$; $P_{CC} = P_C$
Mechanical mixture	$P_{AA} = P_{BB} = P_{CC} = 1$

To determine the type of interstratification in a sample, it is theoretically, necessary only to determine the above probabilities from the Fourier transforms. This can be done with the use of the following statistical relationships where h represents the height of the peak designated by the subscript.

$$h_A = P_A$$

$$h_{AA} = P_A P_{AA}$$

$$h_{AB} = P_A P_{AB} + P_B P_{BA}$$

$$h_{AAB} = P_A(P_{AA}P_{AB} + P_{AB}P_{BA}) + P_B(P_{BA}P_{AA}) + P_C(P_{CA}P_{AB} + P_{CB}P_{BA})$$

In practice, however, it is desirable to try and match all the observed peaks with those calculated for the chosen situations.

In these calculations one should keep in mind the possible existence of structures which cannot be fully represented by this nearest neighbor approach. For example, in a long range structure AABAAB ----, in which $P_{AB} = 0.5$, $P_{BA} = 1$, one would calculate $h_{AAB} = 0.67$, when actually the height is one. However, one may deduce the presence of such long range ordering by observation of the large spacing combination peaks such as AAB, AABB, AAAB, ---- on the Fourier transforms.

Results:

In determining the interstratification of the Belly River bentonite mixed-layer clays the formulae outlined above have been used, and series of peak heights for specific situations calculated* and matched to the observed peak heights. In addition visual examination of the transforms, especially the combination peaks have been used.

Sample 4156:- The transforms for the untreated sample (Figure 6) shows prominent AB, AAB, ABB peaks suggesting a long range ordering of this type. Examining table 14, it is seen that the calculated values for both maximum alternation and randomness do not agree with those observed. The transforms for the glycolated sample (Figure 6) similarly show strong combination peaks of type AC, AAC and ABB, again suggesting a tendency toward a long range ordering. The calculated values (table 14) for maximum alternation and randomness also show poor correlation with the observed peaks.

---

* For the schemes of probability coefficients used in the calculation of the peak heights the reader is referred to Appendix E.

It appears, therefore, that the sample has a long range ordering of type AC, AAB, ACC, - - - - for which calculated and observed peak heights would not be expected to agree.

TABLE 14. OBSERVED AND CALCULATED FOURIER TRANSFORM PEAK HEIGHTS FOR SAMPLE 4156

UNTREATED				GLYCOLATED			
Peaks	Observed Heights	Calculated Heights		Peaks	Observed Heights	Calculated Heights	
		Maximum alternation	Random			Maximum alternation	Random
A	.57	.57	.57	A	.55	.55	.55
B	.43	.43	.43	B	.16	.16	.16
A^2	.17	.14	.32	C	.29	.29	.29
AB	.54	.86	.49	A^2	.25	.10	.30
B^2	.27	.00	.19	AB	.11	.32	.18
A^2B	.37	.65	.42	B^2-AC	.79	.58	.35
AB^2	.61	.32	.32	A^3-BC	.28	.02	.26
				C^2-A^2B	.00	.48	.23
				AB^2-A^2C	.70	.20	.17
				A^4-ABC	.29	.17	.25

Sample 4154:- Examination of the Fourier transforms for the untreated sample (Figure 6) shows high peaks at AB and ABB similar to sample 4156. The calculated and observed heights of the transform for the glycolated sample (table 15) do not show good agreement. The transform (figure 6) has high combination peaks at AC, AAC and ABB, again suggesting a long range ordering.

TABLE 15. OBSERVED AND CALCULATED FOURIER TRANSFORM PEAK HEIGHTS FOR SAMPLE 4154

UNTREATED				GLYCOLATED			
Peaks	Observed Heights	Calculated Heights		Peaks	Observed Heights	Calculated Heights	
		Maximum Alternation	Random			Maximum Alternation	Random
A	.62	.62	.62	A	.59	.59	.59
B	.38	.38	.38	B	.14	.14	.14
A^2	.19	.24	.38	C	.27	.27	.27
AB	.50	.76	.47	A^2	.19	.18	.35
B^2	.00	.00	.15	AB	.05	.28	.17
A^2B	.62	.68	.41	B^2-AC	.81	.54	.34
AB^2	.15	.23	.25	A^3-BC	.31	.05	.29
				C^2-A^2B	.00	.22	.22
				A^2C-AB^2	.76	.43	.32
				A^4-ABC	.36	.02	.26

Sample 4138:- The transform of the untreated sample (Figure 7) has large combination peaks at AB, AAB and ABB, again suggesting long range ordering. Neither of the calculated series of peaks (table 16) show good agreement with those observed. Similarly, the transform (Figure 7) of the glycolated sample has large composite peaks at AB, AC, AAB, AAC and ABB, and neither of the calculated series of peaks (table 16) show good agreement with observed values.

The mixed layer clay in sample 4138 therefore appears to have a long range ordering of the type AB, AC, AAB, AAC, ABB, - - - -.

TABLE 16. OBSERVED AND CALCULATED FOURIER TRANSFORM PEAK HEIGHTS FOR SAMPLE 4138

UNTREATED				GLYCOLATED			
Peaks	Observed Heights	Calculated Heights		Peaks	Observed Heights	Calculated Heights	
		Maximum Alternation	Random			Maximum Alternation	Random
A	.53	.53	.53	A	.50	.50	.50
B	.47	.47	.47	B	.35	.35	.35
A^2	.15	.06	.28	C	.15	.15	.15
AB	.47	.94	.50	A^2	.09	.00	.25
B^2	.38	.00	.22	AB	.32	.91	.35
A^3	.00	.01	.15	B^2-AC	.43	.30	.27
A^2B	.31	.10	.38	A^3-BC	.04	.00	.24
AB^2	.52	.42	.36	C^2-A^2B	.21	.35	.55
B^3	.15	.00	.10	A^2C-AB^2	.46	.40	.41
				A^4-ABC	.03	.21	.21

Sample 4132:- The transform of the untreated sample (Figure 7), as mentioned earlier, cannot be used. Examining the transform of the glycolated sample, (Figure 7), the high combination peaks at CC + AAB and ABB + ACC stand out. None of the calculated arrangements (table 17) check with the observed peaks. It must, therefore, be assumed that a long range ordering of the taype AAB, ABB, AAC, - - - - is present.

TABLE 17. OBSERVED AND CALCULATED FOURIER TRANSFORM PEAK HEIGHTS FOR SAMPLE 4132

GLYCOLATED				
Peaks	Observed Heights	Calculated Heights		
		Maximum Alternation	Random	Mechanical Mixture
A	.20	.20	.20	.20
B	.18	.18	.18	.18
C	.62	.62	.62	.62
A^2	.31	.00	.04	.20
AB	.05	.00	.09	.00
B^2-AC	.21	.40	.57	.18
A^3-BC	.20	.36	.23	.20
C^2-AB	.61	.24	.39	.62
AB^2-A^2C	.46	.06	.16	.00
A^4	.00	.00	.00	.20

This arrangement, however, does not account for the large amount of component C (montmorillonite) present. It therefore appears that a large part of this component is present as a mechanical mixture.

Indexing of Large Spacing Minerals

Theory and Method:

The occurrence of the large spacing clay minerals aroused curiosity as to their nature. The possibility that the large spacings represented a combination of clay lattices so united as to be acting as single crystals was tested by an attempt to index the minerals. Ito's method, or the reciprocal lattice method, as described in detail by Azaroff and Buerger (1958), was used in this study. This method is based on the relationship:

$$Q_{hkl} = h^2a^{*2} + k^2b^{*2} + \ell^2c^{*2} + 2hka^*b^*\cos\gamma^* + 2k\ell b^*c^*\cos\alpha^* + 2\ell hc^*a^*\cos\beta^*$$

$$\text{with } Q_{hkl} = \sigma^2_{hkl} \text{ and } Q_{hkl} = 1/d^2_{hkl}$$

where σ_{hkl} is the reciprocal-lattice vector and a*, b*, c*, α*, β*, and γ* are the reciprocal lattice dimensions.

In indexing a mineral, a series of Q_{hkl} values are determined for the observed d spacings, and these are matched with a series of calculated Q_{hkl} values for a postulated lattice structure. The observed d spacings for the long spacing minerals were taken from combined powder camera and orientated clay data. All possible spacings were listed.

The postulated lattice structure was chosen by consideration of: a) published values for montmorillonite, illite, and vermiculite, b) the observed position of the large apparent 001 reflection, and c) the position of the 060 line. The cell parameter chosen were;

$a_o = 5.2$ Å $\qquad \beta = 95°$

$b_o = 9.0$ Å $\qquad \alpha = 90°$

$c_o = 26.0$ Å $\qquad \gamma = 90°$

The calculations were done by W. Lee using the University of Alberta IBM 1620 computer. The results of the calculations for sample 4156 are tabulated in table 18.

Discussion of Results:

The difference tolerated between the observed and computed Q values was .0025. This was considered to be as accurate as the observed d spacings would allow. With this rejection limit, all peaks were indexed, most of them with several possibilities.

Reconsideration of the problem has led to the conclusion that in as much as the interlayering of the clay components is not regular, the reflections will be apparent, not true lattice reflections, and, therefore, a treatment of the mineral in this way is not warranted. The apparent success of the

indexing in this light can be attributed to the complexity of the components of the mixed-layer clays and the presence of other clay minerals in the sample giving rise to a very large number of reflections. With the large tolerance used most of these reflections will statistically be matched to some possible (hkl) value. Noticable is the indexing of all the kaolinite peaks as minor reflections of the hypothetical lattice. For instance the strong 001 kaolinite peak has been indexed as the reflection from the (012) plane of the postulated lattice.

TABLE 18. INDEXING RESULTS FOR SAMPLE 4156

I	d (Å)	(hkl)**	ΔQ*	I	d (Å)	(hkl)**	ΔQ*
	27.60000				2.00000	$(0\bar{4}\bar{6})$	-.0012
	25.80000	(001)	.0000	20	1.979000	$(\bar{1}\bar{3}\bar{8})$	+.0012
	12.44000	(002)	+.0005	20	1.81200	$(\bar{2}\bar{1}\bar{9})$	-.0010
	11.94000			20	1.70000	$(\bar{3}\bar{1}2)$	+.0001
	11.78000				1.67400	$(\bar{2}\bar{3}9)$	-.0007
	11.62000			20	1.64900	$(\bar{2}\bar{4}\bar{3})$	-.0001
	11.47000				1.62700	$(\bar{3}\bar{1}6)$	-.0002
	11.22000			20	1.53800	$(\bar{3}\bar{2}\bar{4})$	-.0015
	9.71000			80	1.49800	$(\bar{3}0,10)$	+.0002
	9.50000	$(0\bar{1}0)$	-.0012	20	1.37600	$(\bar{1}\bar{6}6)$	+.0006
	7.06000	$(0\bar{1}\bar{2})$	+.0018	20	1.34100	$(\bar{3}\bar{3},10)$	-.0005
25	7.02000	$(9\bar{1}2)$	+.0020	40	1.29600	(400)	-.0009
50	5.50000			25	1.24800	$(\bar{4}\bar{2}1)$	+.0001
	4.89700	$(\bar{1}02)$	+.0011	10	1.20000	$(\bar{4}\bar{1}\bar{6})$	+.0010
100	4.45800	$(\bar{1}\bar{1}1)$	+.0005	10	1.18000	$(\bar{4}\bar{1}\bar{7})$	+.0002
	4.27000	$(\bar{1}0\bar{3})$	+.0003	5	1.15500	$(\bar{1}\bar{7}\bar{8})$	+.0016
20	4.22700	$(\bar{1}04)$	+.0001	5	1.12100	$(0\bar{8}\bar{2})$	-.0003
15	3.53100	$(\bar{1}\bar{1}5)$	-.0002	5	1.10300	$(\bar{4}\bar{4}\bar{3})$	-.0008
90	3.33600	$(\bar{1}\bar{2}2)$	-.0002	5	1.08200	$(\bar{1}\bar{8}\bar{4})$	-.0023
	3.16000	$(\bar{1}07)$	-.0011	5	1.04600	$(\bar{1}\bar{8}8)$	+.0016
5	3.12900	$(0\bar{2}6)$	-.0009	5	1.03700	$(\bar{4}\bar{4}\bar{8})$	-.0008
<5	2.82900	$(0\bar{3}\bar{3})$	+.0004	5	1.01400	$(\bar{5}\bar{1}7)$	+.0010
90	2.56200	$(\bar{1}\bar{3}2)$	+.0006	5	0.98080	$(\bar{1}9\bar{1})$	-.0005
20	2.45300	$(\bar{1}\bar{3}\bar{3})$	+.0005	5	0.96890	$(\bar{5}\bar{2},10)$	+.0001
20	2.37800	$(\bar{1}\bar{3}\bar{4})$	-.0006	5	0.96130	$(\bar{1}\bar{9}6)$	-.0010
<5	2.26900	$(\bar{1}\bar{3}6)$	.0000	5	0.91580	$(\bar{5}\bar{4}9)$	+.0009
20	2.23600	$(\bar{2}\bar{1}6)$	+.0005	5	0.89810	$(\bar{5}\bar{5}0)$	-.0005
20	2.12500	$(0\bar{4}\bar{4})$	+.0001	5	0.88900	$(\bar{2}\bar{9}\bar{8})$	+.0001
	2.03000	$(\bar{1}\bar{4}\bar{2})$	-.0007	5	0.86680	$(\bar{6}03)$	-.0006
	2.01000	$(\bar{2}09)$	+.0011	5	0.79210	$(\bar{4}\bar{9}3)$	-.0002
				5	0.79000		

I = Relative intensities from powder camera data.
** Only (hkl) value with lowest tolerance given.
*ΔQ = Observed Q minus calculated Q.

X-RAY SPECTROCHEMICAL ANALYSIS

General Statement

Recent developments in instrumentation have enabled fluorescence equipment to analyse for elements as light as Mg (Z=12). Thus all major rock forming elements, with the exception of Na, may now be quantitatively determined by this rapid, non-destructive method. The clay minerals under study in this thesis were analysed for the major rock forming elements (excepting Na) in a manner similar to that employed by Molloy and Kerr (1960).

X-ray Fluorescence

Theory and Instrumentation:

Basic X-ray fluorescence theory is given by Webber (1957, 1959) and others. The function of counters and the pulse height analyser are presented in detail by Kiley (1960). Standard Norelco equipment used in this work for manganese and light elements included a tungsten X-ray tube, collimeter, vacuated X-ray path, flow proportional counter for methane-argon (P10) gas, ammonium dihydrogen phosphate (ADP) analysing crystal, pulse height analyser and a strip chart recorder.

For elements heavier than manganese the X-ray path was not vacuated, a scintillation counter and lithium fluoride (LiF) analysing crystal were used, and the pulse height analyser was wide open.

Sample Preparation

Several techniques for sample preparation are presently available (Claisse (1960)). For the present study a technique now in use in the

Department of Geology at the University of Alberta was employed. The samples used for standards were ground for 1 1/2 to 3 hours in acetone with a mechanical mortar to sufficiently reduce the particle size. The samples for analysis were separated from the field samples by sedimentation techniques, and thus only 2 μ to 1/2 μ size material was present. Once the grain size was considered sufficiently fine, about 1 1/2 grams of sample were diluted 1:1 with borax, and this mixture ground in a mechanical mortar with acetone for 15 to 20 minutes. The preparation was then put in a 1 1/4 inch diameter cylinder, backed with 1 to 2 grams of borax, and compressed at 15,000 lbs. per square inch for three minutes.

Calibration Procedure

General Statement:

In X-ray fluorescence analysis, quantities are not measured directly, but must be determined by intensity comparisons between the unknowns and standard samples that have been previously analysed by other techniques. An initial scan is made to ascertain which elements are present and this is followed by detailed measurement of the individual peak heights.

Standards Used:

Due to interference effects, discussed below, standard samples used for calibration should be as close in composition and structure to the unknowns as possible. This is especially true for the complex compounds encountered in clay analysis. A series of clays analysed by wet chemical techniques by Kerr et al (1951) for API (American Petroleum Institute) Research Project 49 were available in the Department of Geology and appeared to be ideal for the purpose. Fourteen of these with varying chemical and

clay mineral content (table 19) were selected, along with one bentonite and one shale analysed in the Department of Geology at the University of Alberta. A number of synthetic samples were also included to determine their suitability for future work of this nature.

Operating Procedures:

Initial scans over the fluorescence spectrum were made in order to determine the elements present. Two scans were made on each unknown and on a borax tablet. The first scan was from 20° 2θ to 87° 2θ at 2° 2θ per minute using the LiF crystal, scintillation counter at 800 volts and P.H.A. wide open. The electronic panel was operated at a scale factor of 256, multiplier 1 and a time constant of 8 seconds. In the second run, the X-ray path was evacuated and the goniometer scanned from 10° 2θ to 60° 2θ at 2° 2θ per minute. The ADP crystal was used, and F.P. counter was operated at 1430 volts with a gas flow of .25 SCFH, and again the P.H.A. was wide open. A scale factor of 4, multiplier 1 and a time constant of 16 were used. Runs on the borax tablet were made to determine instrument background.

In order to keep instrument drift to a minimum, the analysis of each element was done separately and on the same day without changing the instrument settings (except for Al and Si which were determined on the same run). Each peak was scanned three to four times to insure reproducability of the intensity.

Calibration Curves:

The instrument conditions pertinent to the quantitative determination of the elements are shown in table 20. In the construction of the calibration curves (figures 9, 10, and 11), peak intensities were plotted against

TABLE 19. CHEMICAL ANALYSES OF STANDARDS.
(Taken from Kerr, et al, 1951; API Research Project 49)

	Kaolinites			
	API 9a Kaolinite	API 12b Halloysite	API 13 Halloysite	API 16a Dickite
SiO_2	46.07%	44.46%	43.98%	45.18%
Al_2O_3	38.07	36.58	38.46	40.46
Fe_2O_3	.33	.36	-----	.06
FeO	-----	.07	.03	-----
MgO	.01	.18	Trace	Trace
CaO	.38	.19	.32	Trace
Na_2O	.27	.01	.14	.16
K_2O	.43	.51	.48	.37
H_2O^+	13.47	13.38	14.59	14.16
H_2O^-	.43	4.05	2.58	.21
TiO_2	.50	.15	.01	-----
P_2O_5		.18		
MnO	-----	-----		.05
SO_3	Trace			
S				
C	-----			Trace
Total	99.96	100.12	100.59	100.65

	Montmorillonites			
	API 11 Mont-morillonite	API 21 Mont-morillonite	API 33a Nontronite	API 34a Hectorite
SiO_2	53.98%	51.18%	39.92%	53.95%
Al_2O_3	15.97	16.30	5.37	.14
Fe_2O_3	.95	2.2	29.46	.03
FeO	.19	.23	.28	-----
MgO	4.47	4.41	.93	25.89
CaO	2.30	2.12	2.46	.16
Na_2O	.13	.17	Trace	3.04
K_2O	.12	.38	Trace	.23
H_2O^+	9.12	8.29	7.00	5.61
H_2O^-	13.06	15.02	14.38	9.29
TiO_2	.08	.28	.08	Trace
P_2O_5				
Li_2O				1.22
MnO	.06	.01	-----	-----
SO_3				
CO_2	-----		------	
C	-----	-----	-----	-----
Total	100.43	100.59	99.88	99.56

TABLE 19 Continued

	API 35 Illite	API 36 Illite	API 27 Montmoril-lonite	API 43 Attapulgite
SiO_2	56.91%	57.41%	58.53%	54.04%
Al_2O_3	18.50	17.96	19.61	9.83
Fe_2O_3	4.99	4.99	3.10	3.53
FeO	.26	.26	.13	.19
MgO	2.07	2.25	2.65	9.07
CaO	1.59	.64	.25	1.69
Na_2O	.43	.15	1.68	.08
K_2O	5.10	5.75	.31	.57
H_2O^+	5.98	6.70	6.21	10.93
H_2O^-	2.86	2.97	7.89	10.00
TiO_2	.81	.82	.12	.32
P_2O_5				
MnO				-----
SO_3				
S				
C				
Total	99.50	99.90	100.48	100.24

	API 42 Mixed Layer	API 38 Mixed Layer	R-18* Bentonite	R-52** Shale
SiO_2	53.43%	67.15%	49.83%	71.16%
Al_2O_3	21.59	15.09	19.77	12.23
Fe_2O_3	1.04	4.29	1.05	3.14
FeO	Trace	1.26	0.66	.76
MgO	4.17	1.55	4.39	2.34
CaO	.53	.11	4.70	.48
Na_2O	.11	.40	.01	.65
K_2O	7.00	2.77	4.81	4.38
H_2O^+	6.67	4.43	4.58	.80
H_2O^-	5.70	1.36	5.22	2.42
TiO_2	.28	.97	.19	
P_2O_5		.09	.26	.37
Li_2O				
MnO		.04	.03	.02
SO_3				
S				
CO_2			3.03	
C				
Total	100.52	99.87	99.56	100.47

*Analysed in Geochemistry Laboratory at the University of Alberta by R. Wells

**Analysed in Geochemistry Laboratory at the University of Alberta by M. Suska

TABLE 20. OPERATING CONDITIONS FOR FLUORESCENCE X-RAY SPECTROCHEMICAL ANALYSIS*

ELEMENT	CRYSTAL	PEAK USED		PEAK LOCATION °2θ	COUNTER				PULSE HEIGHT ANALYSER		RECORDING CONDITIONS Scale factor—Multi-plier—Time constant
			ORDER		TYPE	VOLTAGE	AMPLIFIER GAIN	GAS FLOW SCFH	BASE LINE V.	WINDOW V.	
26 Fe	LiF	Kα1 Kα2	1 1	57.5	Sci.	800	0	--	--	--	API clays: 512-1-8
25 Mn	ADP	Kα1 Kα2	2 2	16.47	F.P.	1300	0	0.25	5.0	3.0	$kMnO_4$:256-1-4 API clays: 1-1-8
22 Ti	ADP	Kα1 Kα2	2 2	32.10	F.P.	1310	0	0.25	4.0	4.0	2% Ti: 16-1-4 API clays: 4-1-4
20 Ca	ADP	Kα1 Kα2	2 2	48.26	F.P.	1400	0	0.25	15.0	5.0	10% Ca: 32-1-4 API clays: 2-1-8
19 K	ADP	Kα1 Kα2	1 1	11.06	F.P.	1430	0	0.25	15.0	10.0	$KMnO_4$: 256-1-2 API clays: 32-1-2
14 Si	ADP	Kα1 Kα2	1 1	54.15	F.P.	1430	0	0.25	6.0	6.0	Si tablet: 32-1-4 API clays: 4-1-4
13 Al	ADP	Kα1 Kα2	1 1	73.33	F.P.	1430	0	0.25	4.5	5.5	Al disc: 32-1-2 API clays: 2-1-8
12 Mg	ADP	Kα1 Kα2	1 1	106.9	F.P.	1430	0	0.25	4.0	5.0	$Mg(ClO_4)_2$: 1-1-4 API clays: 1-1-8

Sci. = Scintilation
F.P. = Flow Proportional
NOTE: When using PHA, circuit must be on differential. When PHA is wide open, circuit is on integral and base line voltage is zero.
* Basic X-ray unit operated at 50 KV, 40 MA.

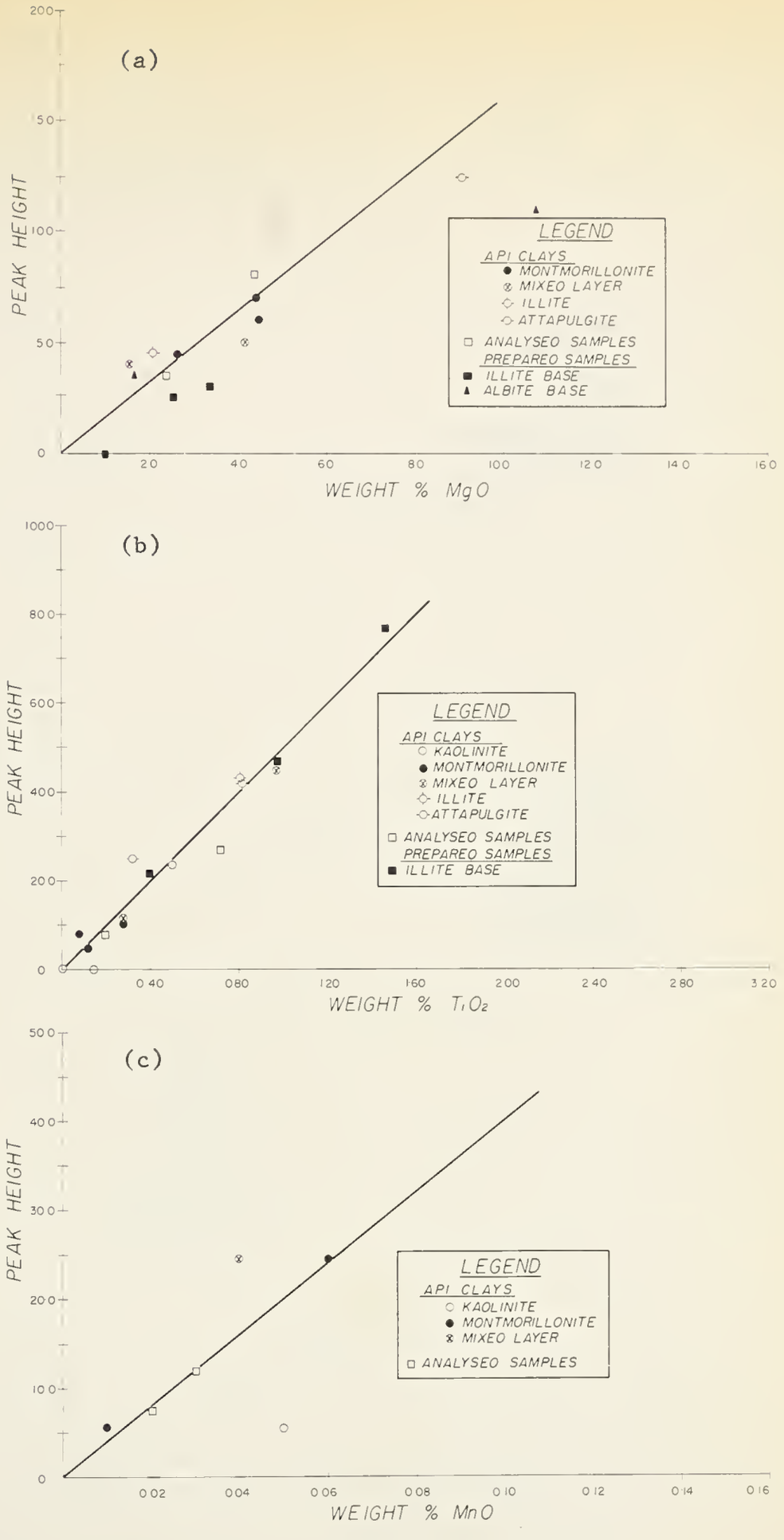

Figure 9. Calibration Curves
a) Magnesium oxide
b) Titanium oxide
c) Manganese oxide

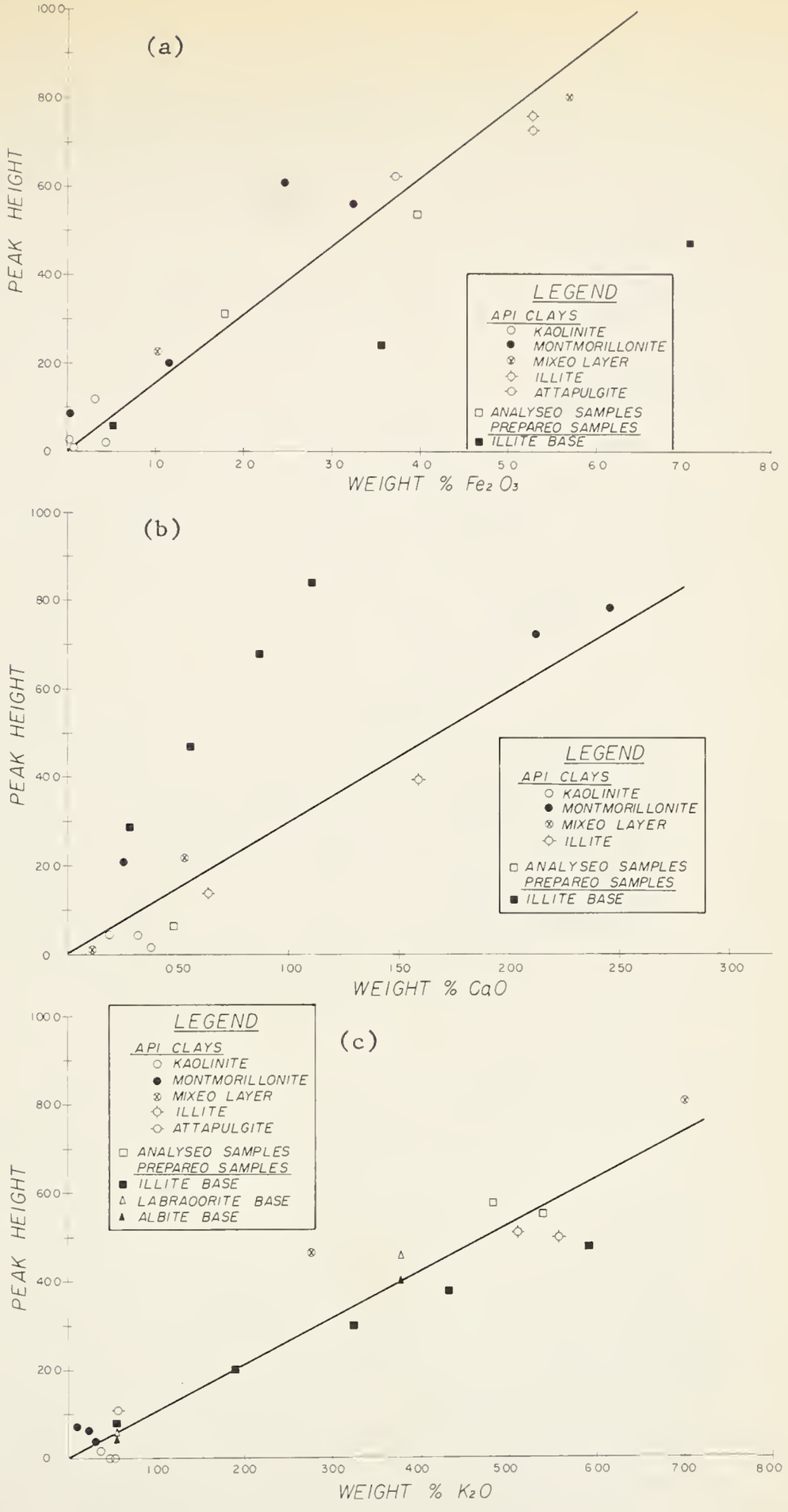

Figure 10. Calibration Curves
a) Iron oxide
b) Calcium oxide
c) Potassium oxide

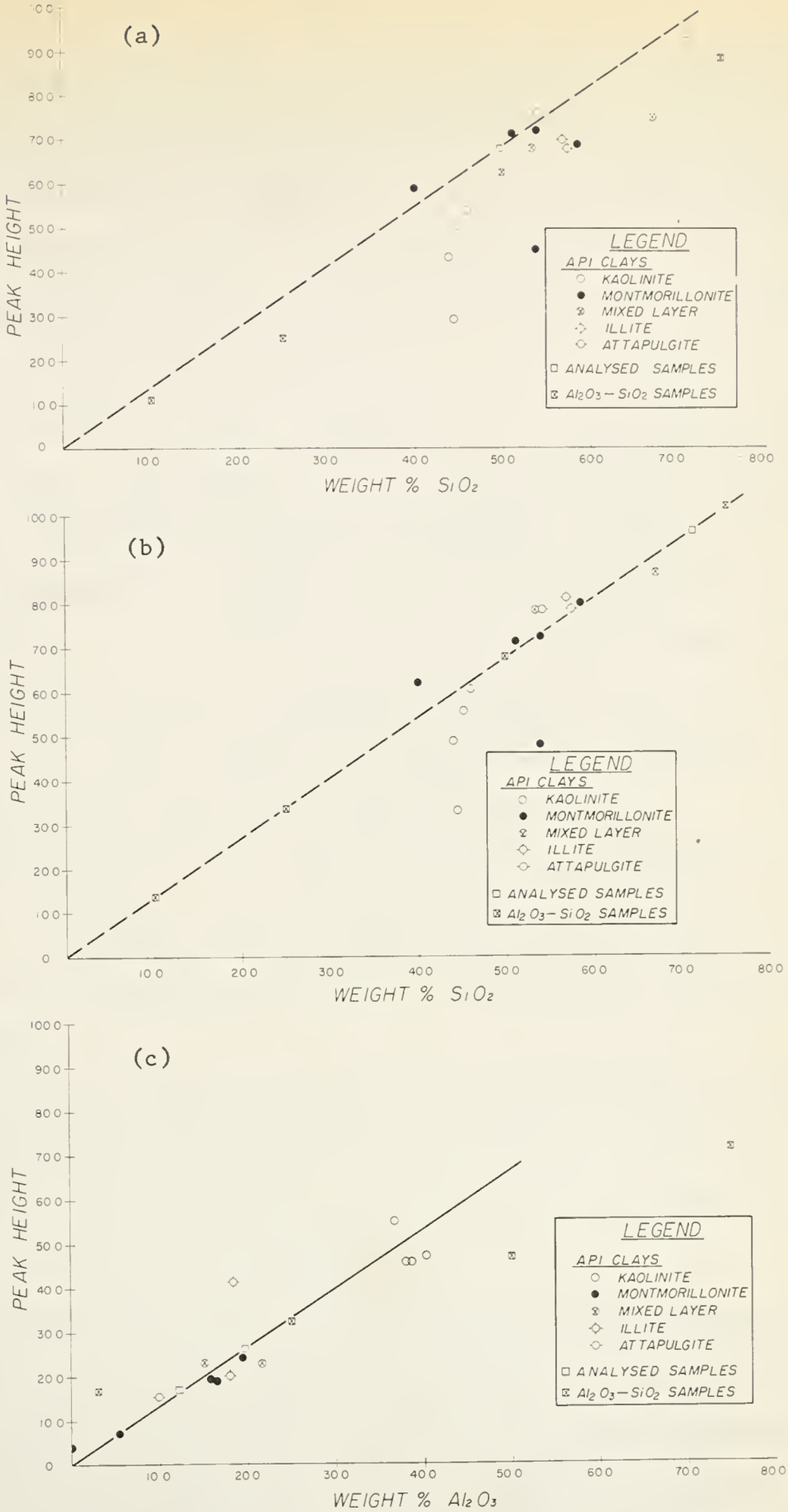

Figure 11. Calibration Curves
a) Silica; peak heights uncorrected for aluminum absorption
b) Silica; peak heights corrected for aluminum absorption
c) Aluminum oxide

weight per cent of the oxide. For each curve the recording conditions used were those given for the API clays in table 20. The curves were drawn as straight lines from the origin, and the slope was determined principally by the values for the API clays and the analysed samples.

The standards plotted on the calibration curves show a considerable scatter that may have several causes:

1. Large amounts of the API standard clays have been collected from the type localities. The samples obtained by the University of Alberta are in some cases quite heterogeneous, and the chemical composition of the samples originally chemically analysed by wet methods could be significantly different from those used as standards in this work. As the analyses were carried out it was suspected that this might be a cause of a large part of the scatter, so two samples analysed in the Rock Analysis laboratory at the University of Alberta were run to check the API clays.

2. The analytical errors to which the wet chemical analysis are subject will also be the cause of some of the scatter, but this may be largely eliminated by the construction of best fit curves from a statistical number of analysis.

3. All prepared samples are subject to weighing, mixing and contamination errors during their preparation. As the present writer did not prepare these standard samples, the care with which they were prepared is not known, and may be the cause of their deviation.

4. The quantitative analysis of an element by X-ray fluorescence depends solely on the measurement of the intensity of the secondary radiation. Thus anything which interferes with this radiation or the primary radiation which activates it will cause an error. Claisse (1960) has considered this problem and suggested four possible error-causing effects; heterogeneity, inhomogeneity, "chemical effect" and inter-element interferences or matrix effect.

From early fluorescence work with powdered samples it soon became apparent that the grain size of the samples effected the intensity. It has since been found that to eliminate this heterogeneity an extremely fine grain size is needed. It was for this reason that lithified or coarse samples were ground in a mechanical mortar with acetone for 1 1/2 to 3 hours. Those separated by sedimentary techniques contained only material in the 2 μ to 1/2 μ size range, and were considered adequately fine.

A more recently discovered effect has been termed inhomogeneity. Elements in different chemical compounds with the same overall composition and uniform grain size were found to give different fluorescence intensities. This effect has been minimized in the present analysis by the use of standards with chemical compounds which are the same or very similar to the clay minerals.

The "chemical effect" is dependent on the dispersion or segregation of atoms in the sample. The more dispersed the atoms, the less the shielding that occurs, and thus the stronger the secondary radiation given off for a given concentration. This effect is minimized by using standards that are structurally similar to the unknowns, that have extremely fine grain size, and by dilution of the samples.

The matrix effect or inter-element interference, is discussed by several authors; Claisse (1960) treats it theoretically, and Molloy (1950) treats it descriptively. This interference is due to the fact that elements absorb radiation at specific wave lengths, and as a result emit characteristic secondary radiation. One element may thus interfere with another in four ways. For example, if element A is the one being measured and B the one interfering, the four possible types of interference are: (1) competitive absorption, when both A and B absorb radiation in the same region; (2) emis-

sion enhancement type A, when both A and B emit radiation in the same region; (3) emission enhancement type B, when B emits radiation in the region where A is absorbing; and (4) emission absorption, when B absorbs radiation in the region where A is emitting. In modern X-ray equipment competitive absorption is eliminated because large excess excitation potential is applied to the sample. There are a number of methods of correcting for the other inter-element interferences. For example, the internal standard method consists of adding a known amount of an element which is influenced by the interfering effects in the same way as the element being analysed. In this way the amount of the interferences is determined. The dilution method will greatly diminish effects due to emission enhancement type B and emission absorption. A pulse height analyser may be used to eliminate emission enhancement type A. In the present work, dilution with borax and a pulse height analyser were employed. However, it was still apparent that some elements were causing emission enhancement type B and emission absorption interferences. Expecially noticable was the Al absorption of Si radiation. A prepared set of Al_2O_3-SiO_2 standards was used to construct a curve showing this interference (figure 12a). A corrected curve passing through the points of minimum absorption is shown in the same figure. A curve for correcting the intensity of the SiO_2 peaks (figure 12b) was constructed in order to eliminate the difference between the two curves in figure 12a. Thus by analysing for Al before Si it is possible to correct the height of the Si peak for Al absorption. Figure 11a shows the Si analysis of the standards before their correction for Al absorption, and figure 11 b shows the same samples after correction.

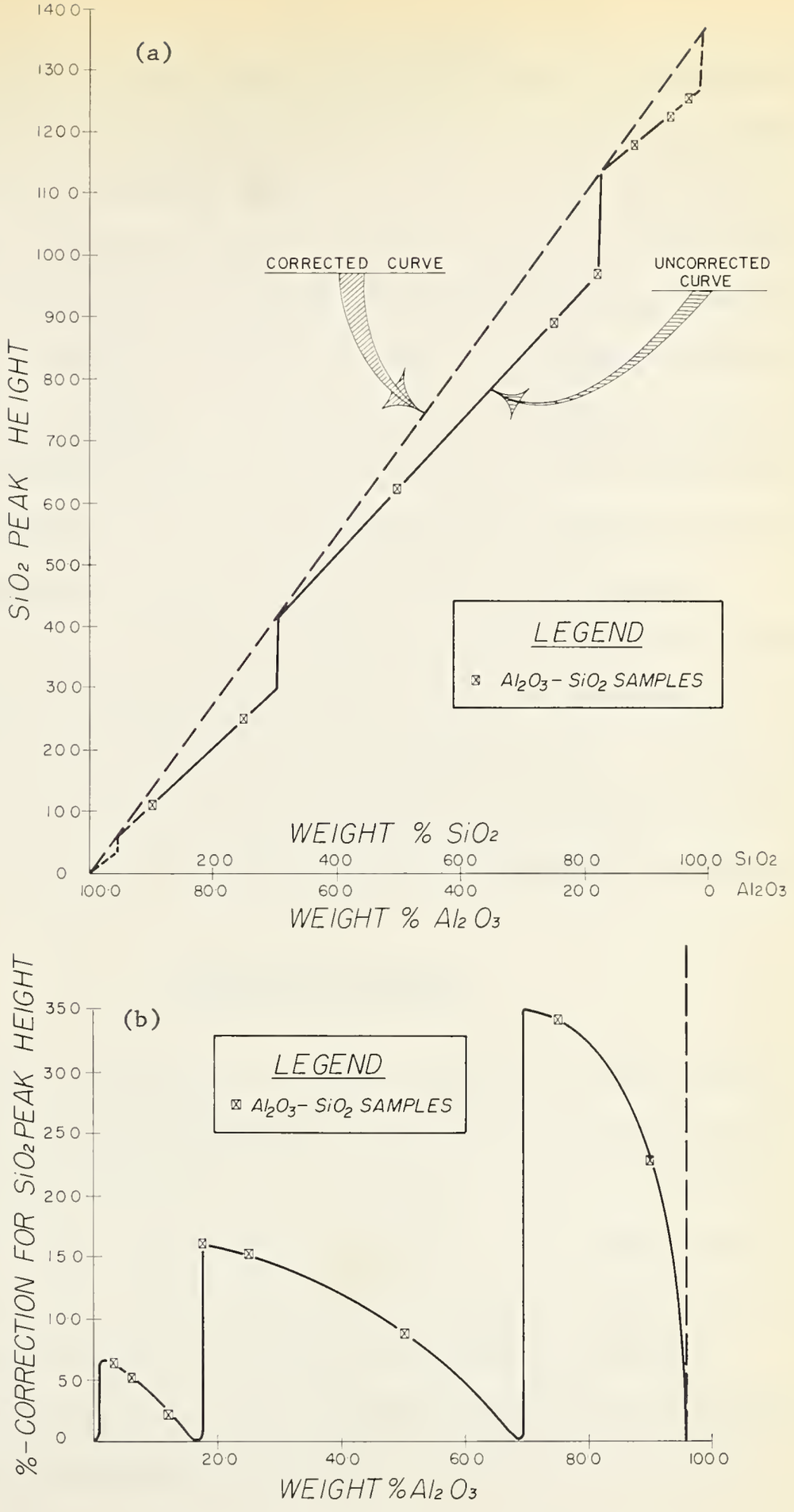

Figure 12. Curves showing effect of absorption of silica emission by aluminum
a) Curve before and after correction
b) Correction curve for silica peak height

One difficulty that arises in the correction for the absorption effect is that some samples have an Al content at an absorption edge, and therefore have two possible correction values. From observations in correcting the calibration curves, it appears that the absorption edge in the vicinity of 18 per cent Al_2O_3 could fall anywhere between 15 and 20 per cent Al_2O_3. For this reason it is difficult to choose the correction for Si peaks in this region. In correcting the standards, the value that gave the best agreement with the corrected curve was used. In the case of the unknowns, both corrections were considered with respect to the sum of the total analysis, and the value giving the best total was used.

The Al absorption of Si radiation while decreasing the Si peaks simultaneously increases the Al peaks. If Al is being measured, this interference can be termed emission enhancement type B. In the present work this interference is not pronounced, but is present, and can be seen on figure 11c where the SiO_2-Al_2O_3 samples diverge from the other standards.

Analysis of Unknowns

Analysis of the unknown samples consisted of taking peak heights and determining the corresponding quantities of oxides from the calibration curves. In the case of Si, the Al absorption correction was made before the percentage was determined from the curve. The results, including the calibrations, have been given in terms of oxides in order to be consistent with accepted methods of presenting rock analyses (table 21).

Elemtns present, but not determinable quantitatively because of the lack of their analysis in the standards are: Ar, Sr, Rb, and Zn.

TABLE 21. CHEMICAL COMPOSITIONS DETERMINED BY X-RAY SPECTROCHEMICAL METHOD

	Bentonites				Shales	
	4156	4154	4138	4132	4134	4133
SiO_2	48.5%	54.5%	60.5%	53.5%	50.0%	55.5%
Al_2O_3	37.5	27.0	22.5	24.0	16.0	16.5
Fe_2O_3	3.85	2.80	4.20	3.90	6.60	7.00
CaO	.66	.85	.97	1.25	1.32	.98
K_2O	4.65	4.65	3.90	3.05	2.30	2.50
MgO	2.20	2.20	2.80	2.80	4.05	3.10
TiO_2	.17	.17	.35	.15	.55	.49
MnO	.03	.02	.02	.05	.09	.10
Total	97.57	92.19	95.24	88.70	80.91	86.17

Comparison of Results with Wet Chemical Analyses

Two the the bentonite samples were chemically analysed by A. Stelmach in the Rock Analysis Laboratory at the University of Alberta, and these analyses along with those obtained for the same samples by the fluorescence X-ray method are presented in table 22. The percentage diviations in part indicate the accuracy of the fluorescence method. SiO_2 analyses show a deviation up to 15% compared to a 3-5% deviation reported by Chodos and Engel (1961). A more serious error appears to be present in the Al_2O_3 analysis where sample 4156 has a 50% deviation as opposed to the 5-10% reported by Chodos and Engel. This unexplained error in aluminum analysis could be the cause of considerable error in the silicon analysis due to the incorrect absorption corrections. Other mean percentage deviations reported by Chodos and Engel are: Fe_2O_3, 3.1; CaO, 1.3; MgO, 3.0; K_2O, 3.2; TiO_2, 3.2; and MnO, 7.7. None of the deviations reported here are within these limits. However, Chodos and Engel, in most cases, were working with considerably larger concentrations, different compounds, and set their curves up with analysed material only.

TABLE 22. COMPARISON OF WET CHEMICAL ANALYSES AND FLUORESCENCE ANALYSES FOR TWO BENTONITES.

	Sample 4156			Sample 4138		
	Wet Chemical	Fluores-cence	Percentage Deviation*	Wet Chemical	Fluores-cence	Percentage Deviation*
SiO_2	52.34	48.4	-7.3	52.73	60.5	+15.
Al_2O_3	24.98	37.5	+50.	23.43	22.5	- 4.7
Fe_2O_3**	4.22	3.85	-8.8	4.34	4.20	- 3.3
CaO	.54	.66	+22.	.80	.97	+21.
K_2O	4.45	4.65	+4.5	3.61	3.90	+ 5.3
MgO	2.3	2.20	-4.3	2.36	2.80	+18.
TiO_2	.19	.17	-9.0	.37	.35	- 5.4
MnO	.01	.03	+200.	.01	.02	+100.
Na_2O	.24	----		.24	----	
P_2O_5	.10	----		.09	----	
H_2O^+	6.63	----		6.16	----	
H_2O^-	4.19	----		5.86	----	
Total	99.89			99.88		

*Deviation of fluorescence analysis from wet chemical analysis.
**Total Fe is reported as Fe_2O_3.
----No analysis.

Although the deviations given above suggest that certain of the elements cannot be very accurately analysed by this fluorescence method, the absolute deviations, excepting those for Al_2O_3 and SiO_2, are low enough that the rapid X-ray fluorescence method of analysis may be considered useful in geological research. These techniques are in the early stages of development and may be expected to become more refined and accurate in the next few years, especially with respect to sample preparation and the establishment of more accurate calibration curves.

CONCLUSIONS

One of the objects of this study was to establish criteria for characterizing the bentonites. The results obtained show that there are no major differences in the clay minerals of the bentonites. However, the lack of montmorillonite as a separate mineral in sample 4156, and its presence in the other three samples along with the higher percentage of kaolinite in 4156 may help to distinguish this bentonite from the other three. The analyses of the mixed layer clays show that samples 4156 and 4154 contain similar amounts of illite, montmorillonite, and vermiculite. In contrasts, sample 4138 has twice as much vermiculite as the first two, and less of both illite and montmorillonite; and sample 4132 has over twice as much montmorillonite as any of the others. This prevalence of interstratified montmorillonite (and correspondingly small amount of illite) along with a large amount of mechanically mixed montmorillonite will probably distinguish bentonite 4132 from the others. Otherwise, the type of interstratification is almost identical in all the samples. All four bentonites are chemically very similar.

The two shales are significatly different from the bentonites both mineralogically and chemically. Both shales lack mixed-layer clays, and contain much larger portions of kaolinite, and smaller portions of illite. Sample 4133 also contains some chlorite. Chemically the two shales are very similar to each other (despite a considerable difference in color), and contain more Fe, Mn, Mg, and Ti, and less K and Al than the bentonites.

Assuming that the environment of deposition of the sediments used in this study was fairly constant, it appears that the source and not the environment was the dominant factor in determining the clays present. The

bentonites, which are chemically very similar and only slightly different mineralogically, suggest similar volcanic sources. Whether the differences noted can be used to distinguish the bentonites must await further work on other samples to see if the differences persist laterally or vary as a result of local environmental conditions. As the shales were deposited in an environment very similar to the bentonites, differences in the clay minerals are due to different source material. The fact that the bentonites and shales were deposited in a similar environment and have retained significant compositional differences supports the conclusion of Weaver (1958a, 1958b, & 1959) that the environment of deposition only slightly modifies the composition of clay minerals.

SELECTED BIBLIOGRAPHY

AZAROFF, L.V. and BUERGER, M.J. (1958): The Powder Method in X-ray Crystallography; McGraw-Hill Book Co., Toronto.

BRADLEY, W.F. (1953): The analysis of mixed-layer clay mineral structures; Analytical Chem., V. 25, p. 727.

---------- (1950): The alternating layer sequence of rectorite; Am. Min., V. 35, p. 590-595.

---------- and WEAVER, C.E. (1956): A regular interstratified chlorite-vermiculite clay mineral; Am. Min., V. 41, p. 497-504.

BRINDLEY, G.W. (1956): Allevardite, a swelling double-layer mica mineral; Am. Min., V. 41, p. 91-103.

BROWN, G. (1961): The X-Ray Identification and Crystal Structures of Clay Minerals; Mineralogical Society (Clay Minerals Group), London.

---------- and MACEWAN, D.M.C. (1950): The interpretation of X-ray diagrams of soil clays, part II; Jour. Soil Sci., V. 1, p. 239-253.

BRUNTON, G. (1955): Vapor pressure glycolation of oriented clay minerals; Am. Min., V. 40, p. 124-126.

BYRNE, P.J.S. and FARVOLDEN, R.N. (1959): The clay mineralogy and chemistry of the Bearpaw Formation of southern Alberta; Research Council of Alberta, Geological Division, Bull. 4.

CHODOS, A.A. and ENGEL, C.G. (1961): Fluorescence X-ray spectographic analysis of amphibolite rocks; Am. Min., V. 46, Nos. 1 and 2, p. 120-133.

CLAISSE, F. (1960): Sample preparation techniques for X-ray fluorescence analysis; Quebec Department of Mines, Laboratories Branch, P.R. No. 402.

EARLEY, J.W., BRINDLAY, G.W., MCVEAGH, W.J. and VANDEN HEUVEL, R.C. (1956): A regular interstratified montmorillonite-chlorite; Am. Min., V. 41, p. 258-267.

---------- and MILNE, I.H. (1956): Regularly interstratified montmorillonite-chlorite in basalt; Clays and Clay Minerals; Nat. Acad. Sci. - Nat. Res. Council Pub. 456, p. 381-384.

FOLK, R.L. (1959): Petrology of Sedimentary Rocks; Hemphill's, Austin, Texas.

GRIM, R.E. (1953): Clay Mineralogy; McGraw-Hill Book Co. Inc., Toronto.

HENDRICKS, S.B. and TELLER, E. (1942): X-ray interference in partially ordered layer lattices; Jour. Chem. Phys., V. 10, p. 147-167.

HENRY, N.F.M., LIPSON, H. and WOOSTER, W.A. (1960): The Interpretation of X-Ray Diffraction Photographs, 2nd ed.; Macmillan Co. of Canada Ltd., Toronto.

JOHNS, W.D., GRIM, C.R. and BRADLEY, W.F. (1954): Quantitative estimations of clay minerals by diffraction methods; Jour. Sed. Petr., V. 24, No. 4, p. 242-251.

JONAS, E.C. and BROWN, T.E. (1959): Three-component interstratifications; Jour. Sed. Petr., V. 29, p. 77-86.

KERR, P.F. et al. (1951): Reference Clay Minerals; American Petroleum Institute Research Project 49. Columbia University, N.Y.

KILEY, W.R. (1960): The function and application of counters and the pulse height analyser; Norelco Reporter, V. VII, No. 6, p. 143-149.

KLUG, H.P. and ALEXANDER, L.E. (1954): X-Ray Diffraction Procedures; John Wiley and Sons Inc., New York.

LANGE (1956): Handbook of Chemistry, 9th ed.; Handbook Publishers Inc., Sandusky, Ohio.

MACEWAN, D.M.C. (1950): Some notes on the recording and interpretation of X-ray diagrams of soil clays; Jour. Soil Sci., VI, p. 90-102.

MCATEE, J.L. (1956): Determination of random interstratification in montmorillonite; Am. Min., V. 41, p. 627 ff.

MOLLOY, M.W. (1959): A comparative study of ten monazites; Am. Min., V. 44, p. 510-532.

---------- and KERR, P.F. (1960): X-ray spectrochemical analysis: an application to certain light elements in clay minerals and volcanic glass; Am. Min., V. 45, Nos. 9 and 10, p. 911-936.

ORR, J.B.B. (1959): Ordovician Bentonites from Ontario; Unpublished M.Sc. thesis, University of Alberta.

SMITH, D.G.W. (1960): Lower Devonian Bentonites From Gaspe Bay, P.Q.; Unpublished M.Sc. thesis, University of Alberta.

WARSHAW, C.M. and ROY, R. (1961): Classification and a scheme for the interpretation of layer silicates; G.S.A. Bull., V. 72, p. 1455-1492.

WEAVER, C.E. (1959): The clay petrology of sediments; in Clays and Clay Minerals, Nat. Acad. Sci.-Nat. Res. Council, p. 154-187.

---------- (1958a): Geological interpretation of argillaceous sediments, part 1; A.A.P.G. Bull., V. 59, p. 91-196.

---------- (1958b): A discussion of the origin of clay minerals in sedimentary rocks; in Clays and Clay Minerals, Nat. Acad. Sci.-Nat. Res. Council, pub. 566, p. 159-173.

---------- (1956): The distribution and identification of mixed layer clays in sedimentary rocks; Am. Min., V. 41, p. 202-221.

WEBBER, G.R. (1959): Application of X-ray spectrochemical analysis to geochemical prospecting; Economic Geology, V. 54, No. 5, p. 816-828.

---------- (1957): Application of X-ray emission spectrometry to rock and ore analysis; Can. Mining and Metallurgical Bull., April, 1957.

APPENDIX A. PROCEDURES FOLLOWED IN SEPARATION OF CLAY SIZE FROM COARSER THAN CLAY SIZE MATERIAL

The field sample, after being weighed air dry, was soaked in distilled water for 1 to 2 days. After the initial soaking the sample was divided into 5 or 6 portions and considerably diluted. These portions were stirred and allowed to settle for 1 hour and 51 minutes after which all the sample above 10 cm. depth was siphoned off and saved. In this length of time all material greater than 4 μ in diameter will settle 10 cm or lower in an aqueous suspension at room temperature (Folk, 1959), and, therefore, the material siphoned off contained only clay size material. This initially decanted clay fraction was that used for the X-ray and chemical analysis work.

In order to concentrate the coarser than clay material, the following procedure was followed. The suspension remaining after the clay sample had been taken was decanted several times with tap water until most of the clay size material was removed. The residue was treated with 20% Muriatic acid (HCl) for four days to two weeks until no visible reaction occurred on further addition of acid. Several dilutions and decantings followed. The remaining sample was then put in a 10% Calgon solution and mixed in a Waring blender for 15 minutes. Further dilutions and decantings followed until material suspended above 10 cm in depth after 1 hour and 51 minutes made the suspension only slightly milky. The coarse fraction remaining was then dried slowly on a hot plate.

APPENDIX B. DATA USED IN CALCULATION OF FOURIER TRANSFORMS.

Sample 4156:

Untreated

Peak (d in Å)	Is	r*(Å^{-1}x100)	$\|Fs\|^2$	θ(s)	i(s)	u(s)
11.4	9.6	8.72	3.3	14.8	19.60	31.5
4.95	1.09	20.2	4.2	6.2	4.20	72.8
3.24	1.67	30.9	7.3	3.9	5.87	111.3

Glycolated

Peak (d in Å)	Is	r*(Å^{-1}x100)	$\|Fs\|^2$	θ(s)	i(s)	u(s)
29.4	18.80	3.40	45.	38.2	1.06	12.25
12.9	3.32	7.76	7.5	16.7	2.67	27.9
9.3	.98	10.75	→0	12.0	~2.00	38.8
5.24	.52	19.10	4.4	6.6	1.79	68.8
3.33	1.19	30.00	6.5	4.0	4.58	108.2

Sample 4154:

Untreated

Peak (d in Å)	Is	r*(Å^{-1}x100)	$\|Fs\|^2$	θ(s)	i(s)	u(s)
11.47	4.42	8.72	3.0	14.6	11.0	31.4
9.1	.22	11.00	→0	11.6	~ .5	39.6
4.95	.51	20.20	4.3	6.5	1.82	72.8
3.39	.54	29.50	6.0	4.1	2.19	106.2
3.20	.46	31.25	7.5	3.8	1.61	112.6

Glycolated

Peak (d in Å)	Is	r*(Å^{-1}x100)	$\|Fs\|^2$	θ(s)	i(s)	u(s)
32.7	16.8	3.06	47.	47.6	.75	11.0
13.0	2.21	7.70	7.0	16.8	1.88	27.7
9.3	.60	10.75	→0	11.8	~1.50	38.8
5.24	.35	19.10	4.4	6.5	1.22	68.8
3.34	.69	30.00	6.5	4.0	2.65	108.0

APPENDIX B Cont.

Sample 4138:

Untreated

Peak (d in Å)	Is	r*(Å^{-1}x100)	$\|Fs\|^2$	θ(s)	i(s)	u(s)
11.6	2.16	8.62	3.7	15.0	3.90	31.1
4.95	.24	20.20	4.2	6.2	.96	72.9
3.18	.41	31.40	7.6	3.8	1.42	113.3
2.56	.22	39.10	.8	2.9	2.00	140.9

Glycolated

Peak (d in Å)	Is	r*(Å^{-1}x100)	$\|Fs\|^2$	θ(s)	i(s)	u(s)
13.4	1.60	5.79	20.0	17.3	.46	26.9
11.6	.48	8.62	4.0	14.6	.82	31.1
5.3	.17	18.52	4.5	6.7	.57	68.0
3.35	.24	29.85	6.4	4.0	.94	107.6

Sample 4132:

Untreated:

Peak (d in Å)	Is	r*(Å^{-1}x100)	$\|Fs\|^2$	θ(s)	i(s)	u(s)
26.0	5.00	3.85	40.	30.2	.41	13.9
12.1	5.30	8.27	4.7	15.6	7.26	29.8
5.0	.20	20.00	4.3	6.2	.75	72.2

Glycolated

Peak (d in Å)	Is	r*(Å^{-1}x100)	$\|Fs\|^2$	θ(s)	i(s)	u(s)
17.0	3.90	5.9	20.	22.0	.89	21.2
5.4	.19	18.5	4.5	6.8	.62	66.8
3.35	.42	29.8	6.4	4.0	1.08	107.5

APPENDIX C. METHOD OF CONSTRUCTION OF THREE COMPONENT COMPOSITION TRIANGLES

The method used is the same that Jonas and Brown (1959) employed in the construction of similar three component triangles. Each triangle is constructed from three two-component systems; one corresponding to each side of the triangle. The migration of the diffraction peaks in these two component systems has been calculated and presented by Brown and MacEwan (1950) and Weaver (1956), except for the 14 Å - 17 Å system. The curve for this system was approximated by drawing a gentle "S" shaped curve similar to the calculated ones. From the calculated curves, peak position scales were marked along the edges of the triangles, and the triangles contoured.

APPENDIX D. EXPANSION OF PROBABILITY COEFFICIENTS

A. n component system

a) $\sum_r Pr=1$

b) $\sum_s Prs=1$ for all r

c) $\sum_r PrPrs=Ps$ for all s

B. Two component (A and B) system

a) $P_A+P_B=1$

b) $P_{AA}+P_{AB}=1$

$P_{BA}+P_{BB}=1$

c) $P_AP_{AA}+P_BP_{BA}=P_A$

$P_AP_{AB}+P_BP_{BB}=P_B$

C. Three component (A, B and C) system

a) $P_A+P_B+P_C=1$

b) $P_{AA}+P_{AB}+P_{AC}=1$

$P_{BA}+P_{BB}+P_{BC}=1$

$P_{CA}+P_{CB}+P_{CC}=1$

c) $P_AP_{AA}+P_BP_{BA}+P_CP_{CA}=P_A$

$P_AP_{AB}+P_BP_{BB}+P_CP_{CB}=P_B$

$P_AP_{AC}+P_BP_{BC}+P_CP_{CC}=P_C$

APPENDIX E. SCHEMES OF PROBABILITY COEFFICIENTS USED IN CALCULATION OF PEAK HEIGHTS FOR FOURIER TRANSFORMS.

Sample 4156:

Untreated

Maximum Alternation		Random	
P_A=.57	P_B=.43	P_A=.57	P_B=.43
P_{AA}=.25	P_{BB}= 0	P_{AA}=.57	P_{BB}=.43
P_{AB}=.75	P_{BA}= 1	P_{AB}=.43	P_{BA}=.57

Glycolated

Maximum Alternation			Random		
P_A=.55	P_B=.16	P_C=.29	P_A=.55	P_B=.16	P_C=.29
P_{AA}=.18	P_{BB}= 0	P_{CC}= 0	P_{AA}=.55	P_{BB}=.16	P_{CC}=.29
P_{AB}=.29	P_{BA}= 1	P_{CA}= 1	P_{AB}=.16	P_{BA}=.55	P_{CA}=.55
P_{AC}=.53	P_{BC}= 0	P_{CB}= 0	P_{AC}=.29	P_{BC}=.29	P_{CB}=.16

Sample 4154:

Untreated

Maximum Alternation		Random	
P_A=.62	P_B=.38	P_A=.62	P_B=.38
P_{AA}=.39	P_{BB}= 0	P_{AA}=.62	P_{BB}=.38
P_{AB}=.61	P_{BA}= 1	P_{AB}=.38	P_{BA}=.62

Glycolated

Maximum Alternation			Random		
P_A=.59	P_B=.14	P_C=.27	P_A=.59	P_B=.14	P_C=.27
P_{AA}=.30	P_{BB}= 0	P_{CC} = 0	P_{AA}=.59	P_{BB}=.14	P_{CC}=.27
P_{AB}=.24	P_{BA}= 1	P_{CA}= 1	P_{AB}=.14	P_{BA}=.59	P_{CA}=.59
P_{AC}=.46	P_{BC}= 0	P_{CB}= 0	P_{AC}=.27	P_{BC}=.27	P_{CB}=.14

Sample 4138:

Untreated

Maximum Alternation		Random	
P_A=.53	P_B=.47	P_A=.53	P_B=.47
P_{AA}=.11	P_{BB}= 0	P_{AA}=.53	P_{BB}=.47
P_{AB}=.89	P_{BA}= 1	P_{AB}=.47	P_{BA}=.53

Glycolated

Maximum Alternation			Random		
P_A=.50	P_B=.35	P_C=.15	P_A=.50	P_B=.35	P_C=.15
P_{AA}= 0	P_{BB}= 0	P_{CC}= 0	P_{AA}=.50	P_{BB}=.35	P_{CC}=.15
P_{AB}=.70	P_{BA}= 1	P_{CA}= 1	P_{AB}=.35	P_{BA}=.50	P_{CA}=.50
P_{AC}=.30	P_{BC}= 0	P_{CB}= 0	P_{AC}=.15	P_{BC}=.15	P_{CB}=.35

Sample 4132:

Untreated

Maximum Alternation			Random		
P_A=.20	P_B=.18	P_C=.62	P_A=.20	P_B=.18	P_C=.62
P_{AA}= 0	P_{BB}= 0	P_{CC}=.39	P_{AA}=.20	P_{BB}=.18	P_{CC}=.62
P_{AB}= 0	P_{BA}= 0	P_{CA}=.32	P_{AB}=.18	P_{BA}=.20	P_{CA}=.20
P_{AC}= 1	P_{BC}= 1	P_{CB}=.29	P_{AC}=.62	P_{BC}=.62	P_{CB}=.18

Mechanical Mixture

P_A=.20	P_B=.18	P_C=.62
P_{AA}= 1	P_{BB}= 1	P_{CC}= 1
P_{AB}= 0	P_{BA}= 0	P_{CA}= 0
P_{AC}= 0	P_{BC}= 0	P_{CB}= 0

APPENDIX F. POWDER CAMERA DATA.

BENTONITE 4156

2θ	d(Å)	RELATIVE INTENSITY	COMMENT
6.2	14.24	~20	Diffuse
7.9	11.18	~20	Diffuse region
9.7	9.11	~20	
12.6	7.02	25	Sharp
16.1	5.500	50	Diffuse region, most intense at higher 2θ
18.1	4.897		
19.9	4.458	100	Hazy
21.0	4.227	20	Hazy
25.2	3.531	15	Hazy - sharp
26.7	3.336	90	Sharp
28.5	3.129	5	Very diffuse
31.6	2.829	< 5	Diffuse
35.0	2.562	90	Diffuse
36.6	2.453	20	Diffuse region
37.8	2.378	20	
39.7	2.269	< 5	Diffuse
40.3	2.236	20	Diffuse region
42.5	2.125	20	
45.8	1.979	20	Very diffuse
50.3	1.812	20	Hazy
53.9	1.700	20	Diffuse
55.7	1.649	20	Very diffuse
60.1	1.538	20	Hazy
61.9	1.498	80	Hazy
68.1	1.376	20	Diffuse
70.1	1.341	20	Very diffuse
72.9	1.296	40	Diffuse
76.2	1.248	25	Very diffuse
79.9	1.200	10	Diffuse
81.5	1.180	10	Diffuse
83.7	1.155	< 5	Diffuse
86.8	1.121	< 5	Very diffuse region
88.6	1.103	< 5	
90.8	1.082	< 5	
94.9	1.046	< 5	
96.0	1.037	< 5	
98.9	1.014	< 5	Diffuse to very diffuse
103.5	0.9808	< 5	
105.3	0.9689	< 5	
106.5	0.9613	< 5	
114.5	0.9158	< 5	
118.1	0.8981	< 5	
120.1	0.8890	< 5	
125.4	0.8668	< 5	
153.0	0.7921	< 5	
154.3	0.7900	< 5	

BENTONITE 4154.

2 θ	d(Å)	RELATIVE INTENSITY	COMMENT
5.5	16.05	~25	Diffuse
7.7	11.47	~20	Diffuse
8.8	10.04	~20	Diffuse
12.4	7.13	20	Sharp
17.8	4.979	60	Hazy
19.9	4.458	100	Sharp
21.0	4.227	5	Diffuse
22.8	3.897	5	Diffuse
25.0	3.559	15	Diffuse
26.7	3.336	50	Very sharp
28.0	3.184	15	Very diffuse region
28.7	3.108	15	
31.3	2.855	10	Diffuse
34.9	2.569	95	Hazy
36.6	2.453	15	Hazy
37.8	2.378	15	Hazy
40.1	2.247	15	Hazy - Diffuse region
42.4	2.130	15	
45.9	1.975	15	
50.2	1.816	5	Sharp
53.9	1.700	15	Hazy
54.8	1.674	15	Extremely diffuse
55.4	1.657		
56.1	1.638		
60.0	1.541	5	Hazy
61.8	1.500	90	Hazy
68.0	1.377	5	Diffuse
69.8	1.346	5	Diffuse
72.9	1.296	25	Hazy
76.2	1.248	20	Diffuse
87.3	1.116	5	All very diffuse
103.4	0.9815	5	
104.9	0.9715	5	
118.3	0.8972	5	
125.5	0.8664	5	

BENTONITE 4138

2θ	d(Å)	RELATIVE INTENSITY	COMMENTS
5.0-5.4	17.66-16.35	50	Diffuse region
7.5	11.78		
10.0	8.84	40	Diffuse
12.4-12.6	7.13-7.02	10-15	Hazy - sharp
15.1	5.862	40	Diffuse region, most of
17.7	5.007		intensity on high 2θ side
19.9	4.458	100	Hazy
21.1	4.207	10	Sharp
25.4	3.504	10	Sharp
26.8	3.324	35	Sharp
28.0	3.184	20	Diffuse
31.4	2.846	5	Diffuse
34.9	2.569	90	Hazy - Diffuse region
36.6	2.453	20	
37.1	2.421	20	
40.4	2.231	20	Hazy - Diffuse region
42.5	2.125	20	
46.1	1.967	20	Very diffuse
50.2	1.816	5	Sharp
53.9	1.700	20	Hazy
55.2	1.663	20	Very diffuse
59.6	1.550	5	Diffuse
61.8	1.500	80	Hazy
67.8	1.381	5	Very diffuse
69.9	1.345	5	Very diffuse
72.9	1.296	30	Hazy
74.5	1.273	5	Diffuse
76.4	1.246	20	Hazy
79.9	1.200	5	--
81.4	1.181	5	--
87.2	1.117	5	Very diffuse
95.9	1.037	5	--
98.4	1.018	5	--
103.4	0.9815	5	Diffuse
105.2	0.9696	5	Diffuse
117.9	0.8991	5	--
119.4	0.8921	5	--
125.4	0.8668	5	Very diffuse

BENTONITE 4132.

2 θ	d(Å)	RELATIVE INTENSITY	COMMENTS
5.2-5.8	16.98-15.22	50	Diffuse
7.7-8.0	11.47-11.04	10	Diffuse
10.1	8.75	20	Very diffuse
12.2-12.5	7.25-7.08	< 5	
15.0	5.901	50	Diffuse region, strongest intensity on high 2θ side
18.4	4.818		
20.0	4.436	100	Diffuse
25.5	3.490	< 5	--
26.7	3.336	5	--
28.6	3.118	10	Very diffuse
31.7	2.820	< 5	--
35.0	2.562	90	Diffuse region
38.3	2.348	10	
40.2	2.241	5-10	Diffuse region
42.9	2.106		
44.4	2.039	5-10	Diffuse region
46.7	1.943		
53.9	1.700	10	Diffuse
55.3	1.660	10	Very diffuse
61.8	1.500	80	Diffuse
73.0	1.295	20	Diffuse
76.4	1.246	15	Diffuse
86.8	1.121	<5	Very diffuse
103.1	0.9835	<5	Very diffuse
105.1	0.9702	<5	Very diffuse
125.6	0.8660	<5	Extremely diffuse